Soluble CD83 Inhibits T Cell Activation by Binding to the TLR4/MD-2 Complex on CD14$^+$ Monocytes

Joe M. Horvatinovich,*[,1] Elizabeth W. Grogan,*[,1] Marcus Norris,* Alexander Steinkasserer,[†] Henrique Lemos,[‡] Andrew L. Mellor,[‡] Irina Y. Tcherepanova,* Charles A. Nicolette,* and Mark A. DeBenedette*

The transmembrane protein CD83, expressed on APCs, B cells, and T cells, can be expressed as a soluble form generated by alternative splice variants and/or by shedding. Soluble CD83 (sCD83) was shown to be involved in negatively regulating the immune response. sCD83 inhibits T cell proliferation in vitro, supports allograft survival in vivo, prevents corneal transplant rejection, and attenuates the progression and severity of autoimmune diseases and experimental colitis. Although sCD83 binds to human PBMCs, the specific molecules that bind sCD83 have not been identified. In this article, we identify myeloid differentiation factor-2 (MD-2), the coreceptor within the TLR4/MD-2 receptor complex, as the high-affinity sCD83 binding partner. TLR4/MD-2 mediates proinflammatory signal delivery following recognition of bacterial LPSs. However, altering TLR4 signaling can attenuate the proinflammatory cascade, leading to LPS tolerance. Our data show that binding of sCD83 to MD-2 alters this signaling cascade by rapidly degrading IL-1R–associated kinase-1, leading to induction of the anti-inflammatory mediators IDO, IL-10, and PGE_2 in a COX-2–dependent manner. sCD83 inhibited T cell proliferation, blocked IL-2 secretion, and rendered T cells unresponsive to further downstream differentiation signals mediated by IL-2. Therefore, we propose the tolerogenic mechanism of action of sCD83 to be dependent on initial interaction with APCs, altering early cytokine signal pathways and leading to T cell unresponsiveness. ***The Journal of Immunology*****, 2017, 198: 2286–2301.**

Human CD83, identified as a 45-kDa type 1 membrane glycoprotein of the Ig superfamily of receptors, is expressed as a membrane-bound form and a soluble form (1, 2). The transmembrane form of CD83 is expressed on mature dendritic cells (DCs), B cells, macrophages, activated T cells and T regulatory cells, and thymic epithelial cells (3, 4). The expression on DCs is involved in the activation of T cell–mediated immune responses (5–8); however, a soluble form of CD83, generated by splice variants or by shedding, inhibits T cell proliferation (9). Soluble CD83 (sCD83) released from tumor cells blocks CD4$^+$ and CD8$^+$ T cell proliferation (10). Additional studies revealed that sCD83 is present in elevated concentrations in a number of hematological malignancies, whereby higher sCD83 plasma levels correlated with shorter treatment-free survival of these patients (11, 12). Released sCD83 from mature DCs infected with CMV leads to inhibition of T cell proliferation (13), and neonatal DC infection with either Gram-negative or -positive bacteria releases sCD83, resulting in suppression of allergic responses (14). These observations prompted several groups to develop recombinant sCD83 proteins (15–17) to evaluate the immunosuppressive activity of sCD83 for therapeutic use in models of autoimmunity and transplantation. Preparations derived from expression of the soluble portion of CD83 lacking the transmembrane domain used in in vivo models of murine and rat kidney and heart allograft transplantation prevented organ transplant rejection (18–20). Moreover, sCD83 induced tolerance in skin allograft transplants (21). In vitro evaluations showed that recombinant CD83 protein preparations inhibits T cell proliferation in vitro (22–24). Moreover, recombinant sCD83 protein reduced the symptoms associated with models of experimental autoimmune encephalomyelitis (25) and murine experimental colitis (26) and, when applied topically, prevented corneal graft rejection (27).

The underlying mechanism by which sCD83 mediates its regulatory properties is not clear. The extracellular domain of CD83 is reported to bind to monocytes and DCs (24, 28), thus positioning CD83 at the interface between innate and adaptive immunity. Published reports suggest that the extracellular domain of CD83 fused to Ig interacts with a 72-kDa glycosylated protein involved in cell adhesion (29); however, this was not investigated further or confirmed by other investigators. Recently, it was indicated that CD83 may act in a homotypic way (30); however, the investigators failed to demonstrate a clear biophysical interaction and, therefore, identification of the sCD83 counterreceptor(s) remains elusive. Identifying the biologically relevant cell surface receptor(s) for sCD83 would greatly expand our understanding of how sCD83 mediates inhibition of T cell activation, alleviates symptoms of autoimmune diseases, and induces tolerance in the allograft transplant setting.

*Research Department, Argos Therapeutics, Inc., Durham, NC 27704; [†]Cancer Immunology, Department of Immune Modulation, University Hospital Erlangen, University of Erlangen-Nuremberg, D-91052 Erlangen, Germany; and [‡]Inflammation and Tolerance Program, Cancer Center, Georgia Regents University, Augusta, GA 30912

[1]J.M.H. and E.W.-G. contributed equally to this work.

ORCIDs: 0000-0001-7187-6729 (A.S.); 0000-0002-9553-6160 (A.L.M.); 0000-0002-2285-9778 (C.A.N.).

Received for publication May 6, 2016. Accepted for publication January 13, 2017.

This work was supported by research funding from Argos Therapeutics, Inc. (to J.M.H., E.W.G., M.N., I.Y.T., C.A.N., and M.A.D.). A.S. was supported by Deutsche Forschungsgemeinschaft Grant DFG-SFB1181 Project B3. A.L.M. was supported by the National Institute of Allergy and Infectious Diseases/National Institutes of Health (Grant AI103347) and the Carlos and Marguerite Mason Trust.

Address correspondence and reprint requests to Dr. Mark A. DeBenedette, Argos Therapeutics, Inc., 4233 Technology Drive, Durham, NC 27704. E-mail address: mdebenedette@argostherapeutics.com

The online version of this article contains supplemental material.

Abbreviations used in this article: DC, dendritic cell; IRAK, IL-1R–associated kinase; MD-2, myeloid differentiation factor-2; MFI, mean fluorescence intensity; sCD83, soluble CD83; TBS-T, TBS with 0.01% Tween 20.

In this study, we identified the cell surface binding partner for sCD83 as myeloid differentiation factor-2 (MD-2), the coreceptor associated with the TLR4 signaling complex. Furthermore, we provide evidence that the expression of CD14 and CD44 on monocytes is a necessary component of this unique complex of receptors. The major role for TLR4 is recognition of pathogen-associated molecular patterns, specifically LPS, from Gram-negative bacteria, which serves as a strong inducer of innate immunity (31–34). LPS signaling through TLR4 requires the coreceptors CD14 and MD-2 because TLR4 does not bind LPS directly (35–37). CD14 first binds LPS and transfers LPS to MD-2, which lacks a transmembrane domain and does not transduce a signal itself, but is responsible for dimerization of TLR4 molecules once bound with LPS (31, 38). The crystal structure of the TLR4/MD-2/LPS complex reveals that LPS binds to a hydrophobic pocket within MD-2 and alters the heterodimerized TLR4 complex (31, 35, 36). Ligand-induced dimerization results in the recruitment of MyD88 and autophosphorylation of members of the IL-1R–associated kinase (IRAK) family (IRAK-1 and IRAK-4), which trigger NF-κB activation via TRAF6 (39–41). TLR4 and IL-1 signaling through IRAK-1 drives proinflammatory cascades relevant to tumorigenesis and serve as a target for antitumor therapy (42). However, antagonist ligands can modulate these adaptor proteins and modulate TLR4 signaling. Evidence for TLR4/MD-2 delivering negative signals is not without precedent. It is a characteristic of high-dose LPS tolerance, in which sustained LPS signaling can lead to immune suppression (43–46). Furthermore, antagonist derivatives of LPS were shown to dampen the proinflammatory cascade associated with sepsis (38). To support our observation that sCD83 interacting with MD-2 alters the TLR4 signaling complex, we provide further evidence that CD44R expressing the v6 variant in the stem loop region expressed on monocytes is an accessory receptor associated with the sCD83–TLR4/MD-2 complex. The contribution of CD44v6 to TLR4/MD-2 signaling is not without precedent. During tissue injury, high m.w. forms of hyaluronan bind to CD44, leading to alternative signaling pathways through the TLR4 complex (44, 47, 48). Furthermore, CD44v6 association with growth factor receptors can induce a feedback loop of regulation mediated by COX-2–induced PGE_2 (49). Taken together, these data provide a mechanism by which highly potent proinflammatory signals can be turned off when no longer required, such as during times of tissue repair and resolution of inflammation.

We report for the first time, to our knowledge, that sCD83 binds directly to MD-2, the TLR4 coreceptor, with high affinity and reveal a novel role for CD44v6 in sCD83 cell surface binding. The mechanism of action driving sCD83 immune regulation is predicated on sCD83 engagement of the TLR4/MD-2/CD14–CD44v6 complex, resulting in a lack of IRAK-1 protein expression. One mechanistic point of LPS tolerance shown in promonocytic THP-1 cells is the rapid degradation of IRAK-1 (50). Furthermore, saponin-like compounds improved clinical outcomes in a mouse model of colitis by blocking IRAK-1 activation and upregulating IL-10 (51). Therefore, we propose that sustained loss of IRAK-1, as a consequence of sCD83 signaling through TLR4, results in the production of PGE_2 and IL-10 and increased IDO activity, which have the combined effect of inhibiting T cell activation. Moreover, we present evidence that sCD83 addition during T cell activation leads to blockade of T cell proliferation and alters cytokine-secretion profiles, rendering T cells unresponsive to further downstream IL-2 expansion. Thus, sCD83 induces a form of IL-2 anergy. Our data support the potential usefulness of sCD83 having therapeutic efficacy to treat autoimmune and inflammatory diseases, as well as alleviate transplant rejection.

Materials and Methods

Preparation of recombinant sCD83 protein

The extracellular domain of human CD83 (20–145 aa) was PCR amplified, and expression of sCD83 was induced in *Escherichia coli* and purified as previously described (16, 24, 52). Briefly, sCD83 was purified using a GSTrap 5-ml column (Amersham Pharmacia Biotech). The GST–sCD83–containing fractions were loaded onto an anion exchange column, and proteins were separated by three different linear salt gradients. The GST–sCD83 fusion protein was incubated with thrombin to separate the sCD83 protein from GST and loaded onto glutathione Sepharose 4B columns. The flow-through containing recombinant human sCD83 protein was collected. A final gel-filtration separation was performed, loading the flow-through onto a Superdex 75 column.

sCD83 binding to peripheral blood monocytes and DCs

Leukapheresis from healthy volunteers was provided by Key Biologics (Memphis, TN). Mononuclear cells were isolated using Histopaque-1077 (Sigma-Aldrich), resuspended in FBS (Atlanta Biologicals) containing 10% DMSO (Sigma-Aldrich), and stored in liquid nitrogen. Thawed PBMCs were washed twice in PBS (Cambrex) prior to use. To detect sCD83 bound to the surface of the cells, sCD83 protein (2 μg) was first incubated with 1×10^6/100 μl of PBMCs resuspended in BD Stain Buffer (FBS; BD Biosciences) for 15 min at room temperature. In some instances, sCD83 protein was incubated with recombinant MD-2 protein (1.5 μg) prior to addition to cells for binding. Goat anti-human CD83 biotinylated polyclonal Ab (R&D Systems) was added to cells incubated with sCD83 and, after washing, allophycocyanin–streptavidin (BD Biosciences) was added to detect sCD83 protein bound to the cell surface of viable cells. For Ab-blocking experiments, cells were incubated with the indicated purified Abs to CD14 (clone M5E2, BD Biosciences; clone 61D3, eBioscience; clone My4, Beckman Coulter), CD44s (clone 515, BD Biosciences; clone IM7, eBioscience; clone 156-3c11, and clone 5F12, Invitrogen), CD44v6 (clone VFF-7; eBioscience), TLR4/MD-2 (clone MTS510; eBioscience), or MD-2 (clone 984, eBioscience; clone 288307, R&D Systems) for 15 min at room temperature prior to the addition of sCD83 protein and subsequent detection of sCD83 bound to the surface of the cell, as described above. Isotype-control IgG1 and IgG2a Abs were purchased from eBioscience. Background staining was determined without the addition of sCD83 protein but in the presence of goat anti-human CD83 biotinylated polyclonal Ab and allophycocyanin–streptavidin. Dead cells were gated using 7-aminoactinomycin D (BD Biosciences). All labeled samples were acquired with an LSR II flow cytometer (BD Biosciences). In the binding-competition experiments to detect direct binding of sCD83 to the surface of cells, sCD83 protein was directly labeled using an Alexa Fluor 488 Protein Labeling Kit (Invitrogen), according to the manufacturer's instructions. To detect surface-bound sCD83 protein and stain cells for CD14, TLR4, MD-2, and CD44v6 expression, mouse anti-CD14 FITC (BD Biosciences) was used to identify monocyte surface CD14, whereas donkey anti-Mouse IgG PE-conjugated Ab (eBioscience) was used to indirectly detect surface TLR4 or MD-2 after binding with sCD83. Detection of sCD83 binding to DCs was performed using the indirect method, as described, in conjunction with anti-CD303 FITC, anti-CD1c PE (Miltenyi Biotec), anti-CD2 Qdot 605, anti CD14-Qdot 655 (Invitrogen), and anti-PE–Cy7 CD123 (BD Biosciences) Abs. Cells were washed, centrifuged, and resuspended in BD Stain Buffer (FBS) containing 7-aminoactinomycin D and acquired with an LSR II flow cytometer. The gating strategy used to detect surface-bound sCD83 protein in combination with conjugated Ab staining is outlined in Supplemental Fig. 1. Sample analysis and positivity based on probability binning were determined using FlowJo software v9.7 (TreeStar). The probability binning algorithm calculates a χ^2 value based on differences in the number of events found in each corresponding bin between the test and control samples.

Cell-free binding assay

sCD83 was prepared at 1 μg/ml in Coating Buffer (OptEIA Reagent Set B; BD Biosciences) and incubated overnight at 4°C. Plates were washed with wash buffer (PBS with 0.05% Tween 20; OptEIA Reagent Set B) three times using an ELx405 auto plate washer, and 300 μl of blocking buffer (1% BSA in PBS) was added to each well. The plates were incubated for 2 h at 37°C to block. After the blocking step, the plates were washed three times with wash buffer. The proteins of interest (MD-2, CD14, MD-2 + LPS, or LPS; R&D Systems, Sigma-Aldrich) were serially diluted in seven tubes, and 100 μl of the diluted protein sample was transferred to the appropriate wells on the capture plate. The plates were incubated for 1 h at room temperature in the dark. Plates were washed, and goat anti-human biotinylated CD83 detection Ab (R&D Systems) was added (100 μl

per well) and incubated for 2 h at room temperature in the dark. The plates were washed, and streptavidin-HRP was prepared at a 1:1000 dilution. Streptavidin-HRP was added (100 μl per well), and the plates were incubated for 1 h at room temperature in the dark. Plates were washed, the development solution was prepared by combining equal parts of Substrate A plus Substrate B (OptEIA Reagent Set B), and 100 μl of solution was added to each well. The plates were allowed to develop for 1–10 min, and the reaction was stopped by adding 50 μl of stop solution (OptEIA Reagent Set B) to each well. The plates were analyzed on a ELx800 universal microplate reader at 450 nm.

Western blotting

Monocytes were isolated from PBMCs using negative selection (STEMCELL Technologies) and cultured in R-10 medium (10% FBS [Atlanta Biologicals], RPMI 1640 supplemented with 10 mM HEPES [pH 7.4], 1 mM sodium pyruvate, 0.1 mM nonessential amino acids, 2 mM sodium glutamate, and 55 mM 2-ME [Invitrogen]) with GM-CSF overnight. sCD83 or LPS was added for the indicated times. Cells were lysed in ice-cold RIPA buffer in the presence of a protease/phosphatase inhibitor mixture (Pierce ECL Plus Western blotting Substrate). Bradford (BCA) protein assay (Thermo Scientific) was performed to determine total protein concentrations. A total of 4–5 μg of each lysate sample was run on each lane of a Criterion 10–20% Tris-HCl gel. The gel was run at 200 V for 50 min. The gel was transferred to a polyvinylidene difluoride membrane at 100 V for 75 min. The membrane was washed in TBS with 0.01% Tween 20 (TBS-T), blocked in 5% nonfat milk in TBS-T for 1 h, and washed three times with TBS-T. The washed membrane was incubated with primary Ab (1:1000; IRAK1, IRAK2, IRAK-M, IRAK4, and TRAF6; all from Cell Signaling Technology) in 3% BSA in TBS-T at 4˚C overnight. The membrane was washed and then incubated with anti-rabbit HRP (1:2000) in blocking buffer for 1 h. The blot was developed using an ECL Plus kit.

T cell stimulation assay

Human PBMCs from normal donors were thawed overnight in R-10 medium. Cells were labeled with CFSE using the CellTrace CFSE Cell Proliferation Kit, for flow cytometry (Life Technologies). CFSE-labeled cells were incubated with various concentrations of sCD83 protein. To stimulate proliferation of PBMCs, anti-human functional grade purified CD3 and CD28 Abs (eBioscience) were added to the wells at a concentration of 0.123 ng/ml, and cells were incubated for 6 d at 37˚C. On day 6, cells were harvested and stained with Abs against CD3 (PECy7; BD Biosciences), CD4 (Pacific Blue; BD Biosciences), and CD8 (PE–Texas Red–X [ECD; Beckman Coulter]) for 15 min at room temperature. LIVE/DEAD Fixable Aqua Dead Cell Stain (Life Technologies) was used as a viability marker. Cells were washed twice with FACS stain buffer (with FBS; BD Biosciences), stained with the Aqua Dead Cell Stain Kit for 15 min at room temperature, and washed twice more with the FACS stain buffer. Fluorescence was measured on an LSR II, and a total of 100,000 events was collected for each sample. Proliferation was measured by the distribution of CFSE in each sample. Fluorescence was measured on an LSR II using FACSDiva software (BD Biosciences). Data were analyzed with FlowJo software.

Detection of cytokine secretion

To evaluate cytokine secretion from stimulated PBMC cultures in response to sCD83 treatment, the supernatant was collected after culture and analyzed for human cytokines using the Cytometric Bead Array kit (BD Biosciences), according to the manufacturer's instructions. Data were analyzed using FCAP Array software (BD Biosciences). PGE_2 concentrations were measured using a competitive ELISA kit (Thermo Fisher).

Detection of intracellular cytokine staining

Expression of IL-10, IFN-γ, and TNF-α by T cells, B cells, and monocytes was analyzed by intracellular cytokine staining. PBMCs were stimulated with anti-CD3/anti-CD28 Abs and treated or not with sCD83 for 24 h. GolgiPlug and GolgiStop (both from BD Biosciences) were added for the final 18 h of stimulation. Twenty-four hours poststimulation, cells were harvested, washed with FACS stain buffer, and stained for 15 min at room temperature with the LIVE/DEAD Fixable Aqua Dead Cell Stain kit. Cells were washed again, and labeled with anti-mouse CD3 allophycocyanin–eFluor 780 (eBioscience), FITC anti-CD4 (BioLegend), BV786 anti-CD8 (BD Biosciences), BV605 anti-CD14 (BD Biosciences), and BV786 anti-CD19 (BD Biosciences) Abs for 15 min at room temperature. Samples were washed twice and fixed with BD Cytofix for 10 min at 4˚C. Cells were washed and resuspended in FACS stain buffer and held overnight at 4˚C. The following day, tubes were washed with Perm/Wash buffer (BD Biosciences). To set background gates, a single tube (blocked tube) containing the blocking Abs (purified anti–IL-2 [BD Biosciences], purified anti–IL-10 [eBioscience], purified anti–IFN-γ [eBioscience], and purified anti–TNF-α [BD Biosciences]) was added to the intracellular cytokine–stained blocking tube for 10 min at room temperature. Anti–IL-2 PE (BD Biosciences), anti–IL-10 PE-Cy7 (eBioscience), anti–IFN-γ eFluor 450 (eBioscience), and anti–TNF-α Alexa Fluor 700 (BD Biosciences) Abs were added to all tubes, and samples were incubated for 15 min at room temperature. Cells were washed twice with Perm/Wash buffer and resuspended in FACS stain buffer for acquisition. Fluorescence was measured on an LSR II using FACSDiva software, and data were analyzed with FlowJo software. Background staining for each individual cytokine Ab was determined by setting the gates on the nonstained cell population present in the blocked tube (Supplemental Fig. 2).

Determination of IDO activity

IDO activity in PBMC cultures was assessed by detecting tryptophan and the tryptophan catabolite kynurenine, which is generated by cells expressing IDO. Kynurenine and tryptophan in culture media were measured by HPLC after deproteination using a C18 reverse phase column, as described (53, 54). Data are expressed as the ratio of kynurenine/tryptophan.

Statistics

Statistical analysis was performed using Microsoft Excel 2016 software version (Santa Cruz, CA) and variances of mean values are presented as box-and-whisker plots. Statistical comparisons of T cell subsets from different donors were calculated using a paired t test. Spearman rho plots were calculated for comparison of mean fluorescence intensity (MFI) values for the cohort of six donors. The p values ≤ 0.05 were considered statistically significant.

Results

sCD83 binds to $CD14^+$ monocytes expressing the TLR4 coreceptor MD-2

PBMCs were incubated with sCD83 protein, and cell surface binding was detected on $CD14^+$ monocytes and $CD19^+$ B cells (Fig. 1A). Forward and side scatter differentiated monocytes from lymphocytes (Fig. 1Ai). There are no detectable $CD14^+/CD19^+$ double-positive B cells in the lymphocyte gate (Fig. 1Aii) or the monocyte gate (Fig. 1Aiii). Within the monocyte gate, 98% of the cells are $CD14^+$, with no detectable $CD19^+$ B cells present (Fig. 1Aiii). sCD83 protein bound to the surface of 38% of the $CD19^+$ B cells (Fig. 1Aiv, open graphs) and 64% of the monocytes (Fig. 1Av, open graphs). However, neither the monocytes nor B cells show positive staining when the secondary anti-CD83 Ab is added to cells in the absence of sCD83 protein; thus, neither cell population expresses membrane-bound CD83 (Fig. 1Aiv, 1Av, shaded graphs). The remaining cells in the lymphocyte gate do not bind sCD83 protein (Fig. 1Avi). To show direct cell binding of sCD83 protein, sCD83 protein was directly labeled with Alexa Fluor 488 dye, and flow cytometry analysis revealed that fluorescent-labeled protein and unlabeled sCD83 protein detected with the indirect biotinylated anti-CD83 Ab bound to the same cells, resulting in 77.9% of the monocytes being double stained with both reagents (Fig. 1B). To confirm specificity of sCD83 binding to monocytes, a competition binding assay was performed. Direct binding of Alexa Fluor 488–labeled sCD83 was inhibited when titered concentrations of unconjugated sCD83 protein were preincubated with the cells, demonstrating sCD83-specific binding to the cell surface of monocytes (Fig. 1C). This prompted us to investigate the binding of sCD83 to other APCs present in PBMCs. Mature DCs present in the peripheral blood (55) were identified by the expression of CD123 and CD303 (plasmacytoid DCs) (Fig. 1D, top panel), and monocyte-derived DCs were identified by the expression of CD1c and CD2 (Fig. 1E, top panel). sCD83 binding could be detected on a subset of $CD14^+$ DCs within the mature plasmacytoid DC subset (38.7%) (Fig. 1D, middle panel) and the myeloid DC subset (68.9%) (Fig. 1E, middle panel). Neither population of DCs expressed surface CD83, as was evident by a lack of staining with the biotinylated

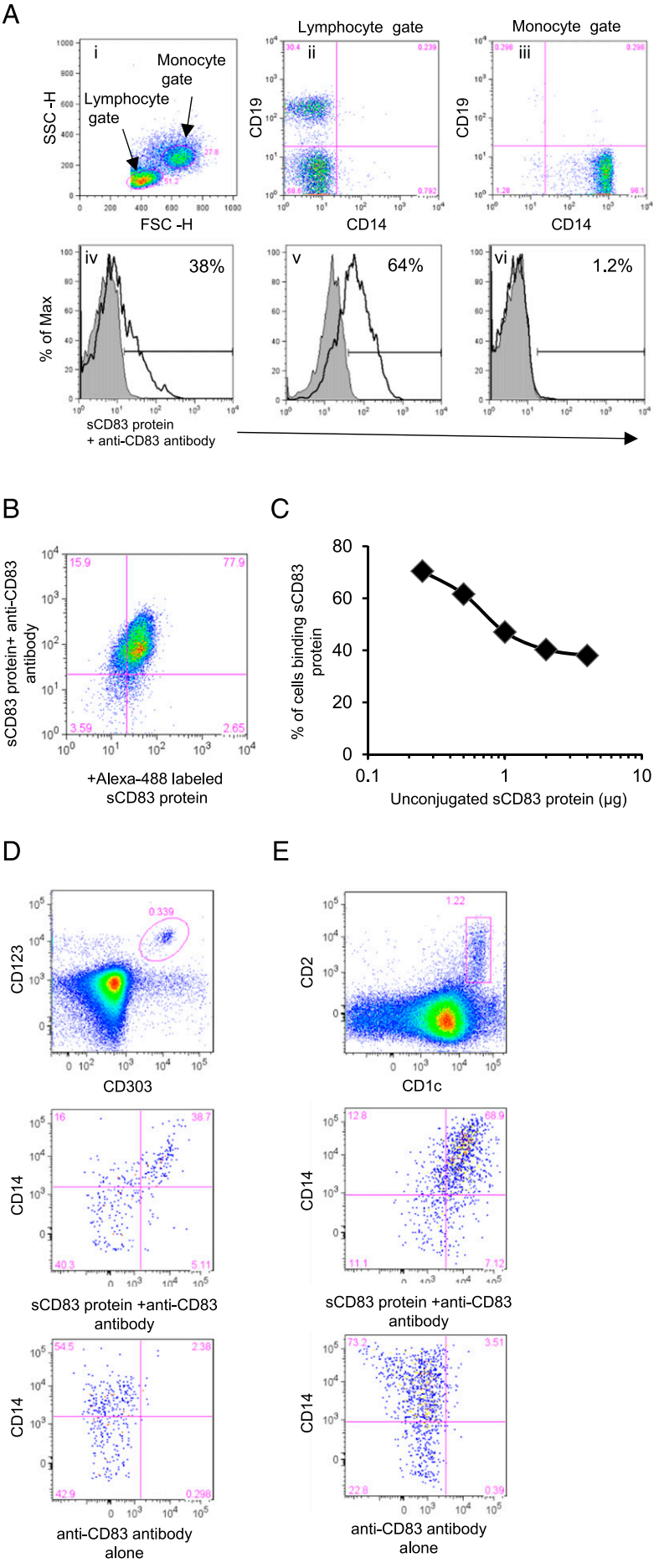

FIGURE 1. Cell surface binding of sCD83 protein. sCD83 protein was added to PBMCs, and binding to $CD14^+$ monocytes or $CD19^+$ B cells was detected using a secondary goat anti-human CD83 biotinylated Ab, followed by allophycocyanin-streptavidin. Gating of viable monocytes and background staining when cells are stained with biotinylated anti-CD83 Ab plus allophycocyanin-streptavidin is shown in Supplemental Fig. 1. (**Ai**) Viable monocytes and lymphocytes were identified by side scatter (SSC-H) and forward scatter (FSC-H) gating. $CD14^+$ cells, representative of monocytes or $CD19^+$ B cells, and $CD14^-/CD19^-$ cells were identified in the lymphocyte gate (**ii**) and monocyte gates (**iii**). Percentages of $CD19^+$ cells in the lymphocyte gate (**iv**), $CD14^+$ cells within the monocyte gate (**v**), and $CD14^-/CD19^-$ cells in the lymphocyte gate (**vi**) binding sCD83 protein (open graphs). Background cell staining is shown with anti-CD83 biotinylated Ab, followed by allophycocyanin-streptavidin in the absence of sCD83 protein (shaded graphs). (**B**) Cells present in the monocyte gate were double stained with both Alexa Fluor 488–conjugated sCD83 protein and the unlabeled protein detected with the anti-CD83 Ab, followed by allophycocyanin-streptavidin. (**C**) To generate a competition binding curve, cells were incubated with various concentrations (0.25 to 4 μg) of unconjugated sCD83 protein for 15 min at room temperature. After incubation, Alexa Fluor 488–labeled sCD83 was added to the cell suspension without prior washing. The percentage of Alexa Fluor 488–labeled sCD83 binding is shown in the presence of various concentrations of unlabeled sCD83. Data are representative of two to five independent experiments. (**D**) Plasmacytoid DCs present in the monocyte gate from a single donor were identified by expression of CD123 and CD303 (top panel). Binding of sCD83 protein to $CD14^+$ DCs within the $CD123^+/CD303^+$ plasmacytoid DC subset was detected using the same two-step method of incubating sCD83 protein with cells then detection with anti-CD83 biotinylated Ab followed by allophycocyanin-streptavidin (middle panel). Background staining in the absence of sCD83 protein but in the presence of the anti-CD83 Ab alone, followed by allophycocyanin-streptavidin (bottom panel). (**E**) Myeloid DCs present in the monocyte gate from a single donor identified by expression of CD1c and CD2 (top panel). Binding of sCD83 protein to $CD14^+$ DCs within the $CD1c^+/CD2^+$ myeloid DC subset was detected as described above using the indirect detection method (middle panel). Background staining in the absence of sCD83 protein (bottom panel).

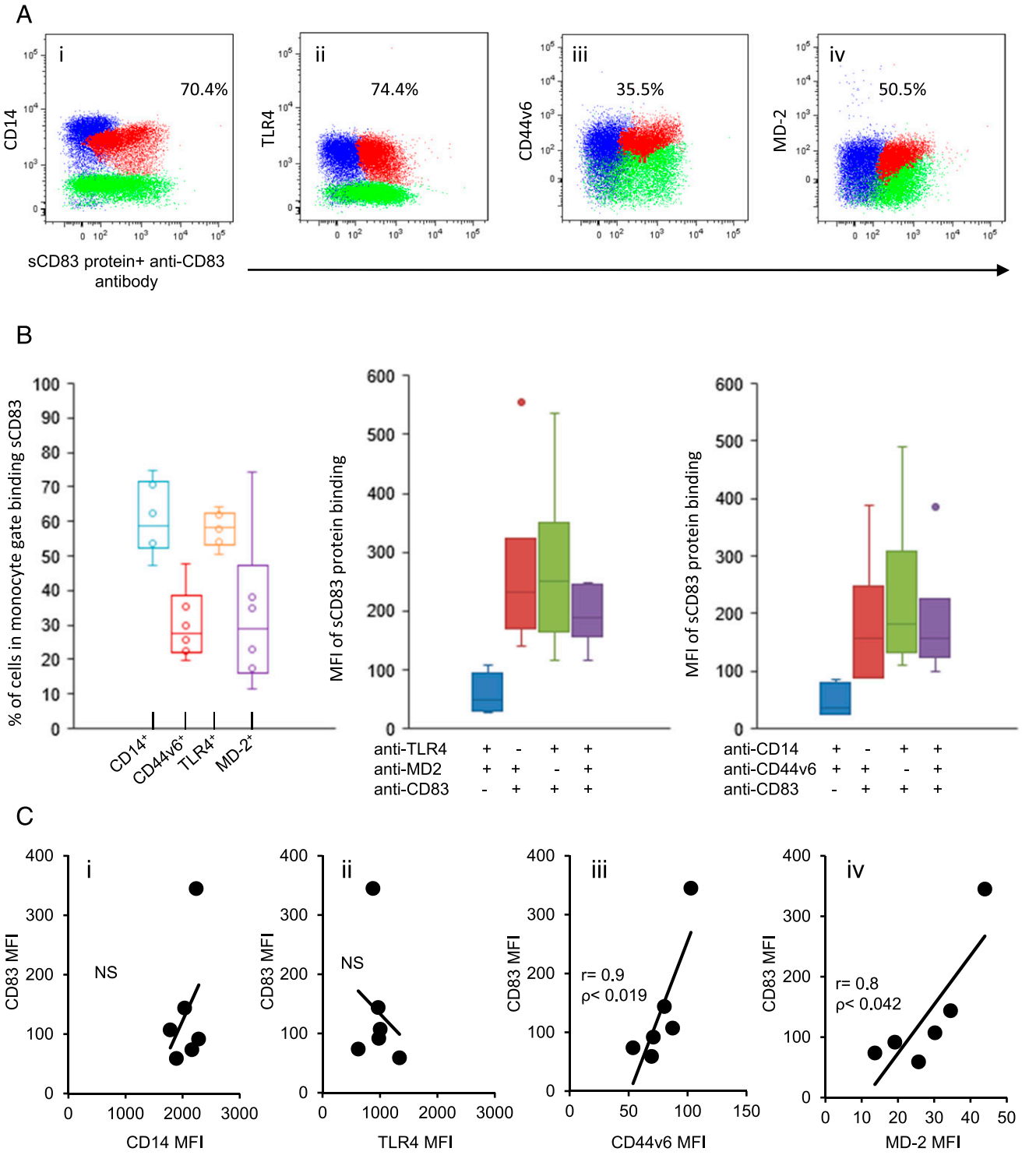

FIGURE 2. sCD83 binds to monocytes expressing CD14/TLR4/MD-2 CD44 coreceptors. sCD83 protein was added to PBMC cultures and detection of surface-bound sCD83 was performed as described in *Materials and Methods*, in combination with staining for expression of CD14, TLR4, CD44v6, and MD-2. (**A**) Representative dot plots showing probability binning to partition data for χ^2 testing based on positive surface binding with CD83 protein in combination with CD14 (**Ai**), TLR4 (**Aii**), CD44v6 (**Aiii**), or MD-2 (**Aiv**) staining. (The gating strategy is shown in Supplemental Fig. 1.) In (Ai), the blue dots represent $CD14^+$ staining in the absence of sCD83 protein, green dots represent cells binding sCD83 protein in the absence of CD14 staining, and the red dots represent cells staining double positive for CD14 and sCD83 binding. In (Aii), the blue dots represent $TLR4^+$ staining in the absence of sCD83 protein, green dots represent cells binding sCD83 protein in the absence of TLR4 staining, and the red dots represent the percentage of cells staining double positive for TLR4 and sCD83 binding. In (Aiii), the blue dots represent $CD44v6^+$ staining in the absence of sCD83 protein, green dots represent cells binding sCD83 protein in the absence of CD44v6 staining, and the red dots represent the percentage of cells staining double positive for CD44v6 and sCD83 binding. In (Aiv), the blue dots represent $MD\text{-}2^+$ staining in the absence of sCD83 protein, green dots represent cells binding sCD83 protein in the absence of MD-2 staining, and the red dots represent the percentage of cells staining double positive for MD-2 and sCD83 binding. (**B**) Box-and-whisker plots show the distribution of the percentage of cells in the monocyte gate binding sCD83 protein into the upper and lower quartiles ($n = 6$) (left panel). The distribution of cells within the monocyte gate that are double positive for sCD83 and CD14 (blue bar), sCD83 and CD44v6 (red bar), sCD83 and TLR4 (green bar), and sCD83 and MD-2 (purple bar) is shown. The level of sCD83 binding, represented by the MFI value, is shown (*Figure legend continues*)

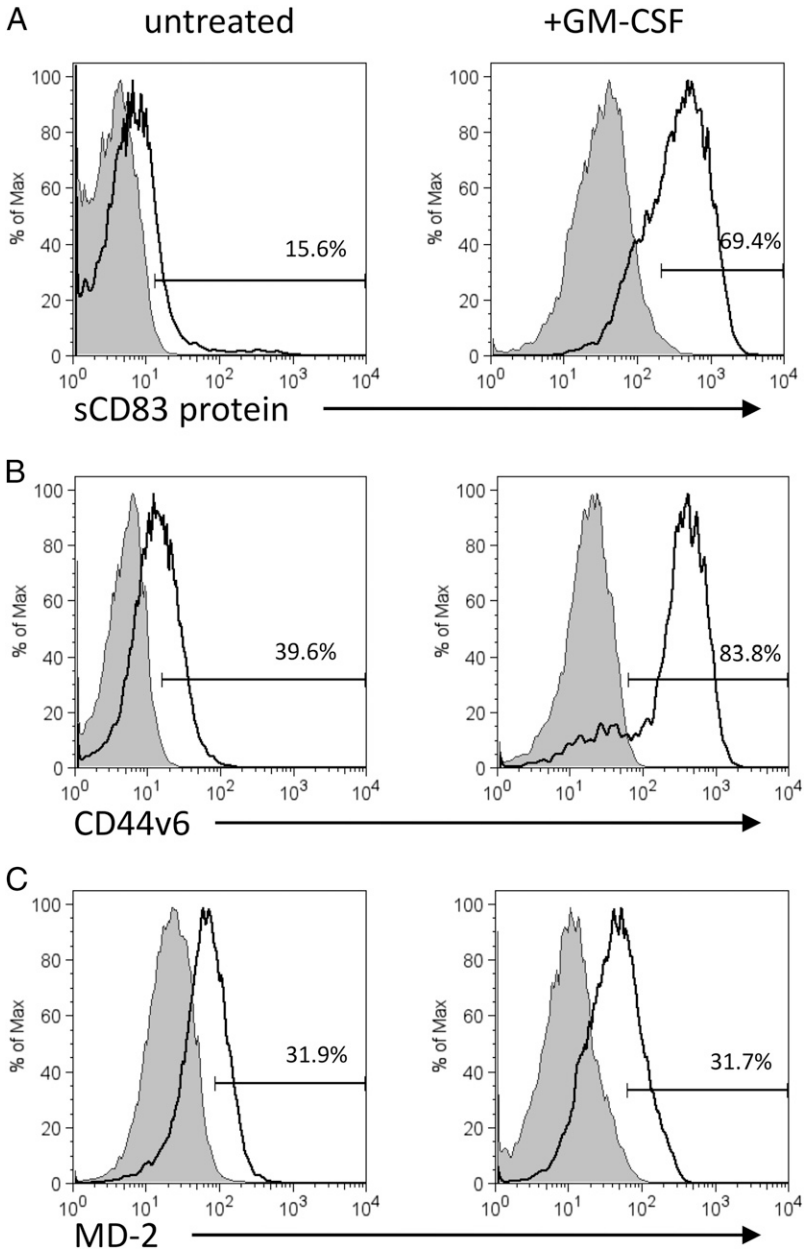

FIGURE 3. GM-CSF enhances sCD83 binding to monocytes expressing high levels of CD44v6. (**A**) sCD83 protein binding to monocytes was determined, as described in *Materials and Methods*, on untreated cells (left panel) or GM-CSF–treated cells (right panel). (**B**) Expression of CD44v6 was determined on untreated cells (left panel) or GM-CSF–treated cells (right panel). (**C**) MD-2 expression was determined on untreated cells (left panel) or GM-CSF–treated cells (right panel). Data shown are representative of three experiments.

anti-CD83 Ab (Fig. 1D, 1E, bottom panels). Both $CD14^+$ DC subsets are present in the monocyte gate and represent a small, but detectable, population of cells with the ability to bind sCD83. In the monocyte gate, 0.13 and 0.84% of cells consisted of sCD83 bound to $CD14^+$ plasmacytoid and monocytic DCs, respectively. To extend these observations, we characterized the phenotype of monocytes binding sCD83. Fig. 2A shows representative data from one of six donors: 70.4% of the $CD14^+$ monocyte population (Fig. 2Ai), 74.4%

for cells multistained for TLR4 and MD-2 (middle panel). The blue bar represents the background MFI value of sCD83 detection when cells are multistained with Abs to detect TLR4 and MD-2 expression without added sCD83 protein (anti-CD83 second step alone). The red bar represents the MFI value of sCD83 binding when cells are double stained to detect MD-2 expression and sCD83 binding. The green bar represents the MFI value of sCD83 binding when cells are double stained to detect TLR4 expression and sCD83 binding. The purple bar represents the MFI values of sCD83 binding when cells are multistained for TLR4 and MD-2 expression in the presence of sCD83 binding. The level of sCD83 binding, represented by the MFI value, is shown for cells multistained for CD14 and CD44v6 (right panel). The blue bar represents the background MFI value of sCD83 detection when cells are multistained with Abs to detect CD14 and CD44v6 expression without added sCD83 protein (anti-CD83 second step alone). The red bar represents the MFI value of sCD83 binding when cells are double stained to detect CD44v6 expression and sCD83 binding. The green bar represents the MFI values of sCD83 binding when cells are double stained to detect CD14 expression and sCD83 binding. The purple bar represents the MFI values of sCD83 binding when cells are multistained for CD14 and CD44v6 expression in the presence of sCD83 binding. (**Ci**) sCD83 binding MFI values plotted versus the CD14 MFI values of cells double positive for sCD83 binding and CD14 expression. (**Cii**) sCD83 binding MFI values plotted versus the TRL4 MFI values of cells double positive for sCD83 binding and TLR4 expression. (**Ciii**) sCD83 binding MFI values plotted versus the CD44v6 MFI values of cells double positive for sCD83 binding and CD44v6 expression. (**Civ**) sCD83 binding MFI values plotted versus the MD-2 MFI values of cells double positive for sCD83 binding and MD-2 expression. Data shown are representative of three independent experiments, and each data point is representative of the average of triplicates for each of six donors from one experiment. Statistics are displayed by Spearman rho plots.

of TRL4$^+$ cells (Fig. 2Aii), 35.5% of CD44v6$^+$ cells (Fig. 2Aiii), and 50.3% of MD-2$^+$ cells (Fig. 1Aiv) bound sCD83. Compiled data from the six donors showed that 47–75% of CD14$^+$ cells, 20–48% of CD44v6$^+$ cells, 50–62% of TLR4$^+$ cells, and 11–75% of MD-2$^+$ cells (Fig. 2B, left panel) bound sCD83. Interestingly, when we investigated the relative level of sCD83 binding by measuring the MFI values of bound sCD83 protein in combination with Ab staining to TLR4 and MD-2, there was a nonsignificant, but trending, decrease in the MFI values of bound sCD83 (Fig. 2B, middle panel, purple bars). A similar pattern of decreased binding of sCD83 protein in combination with Ab staining to CD14 and CD44v6 was observed (Fig. 2B, right panel, purple bars). This prompted us to investigate the relationship between the level of expression of CD14, TLR4, MD-2, or CD44v6 and the level of sCD83 protein bound to the cell

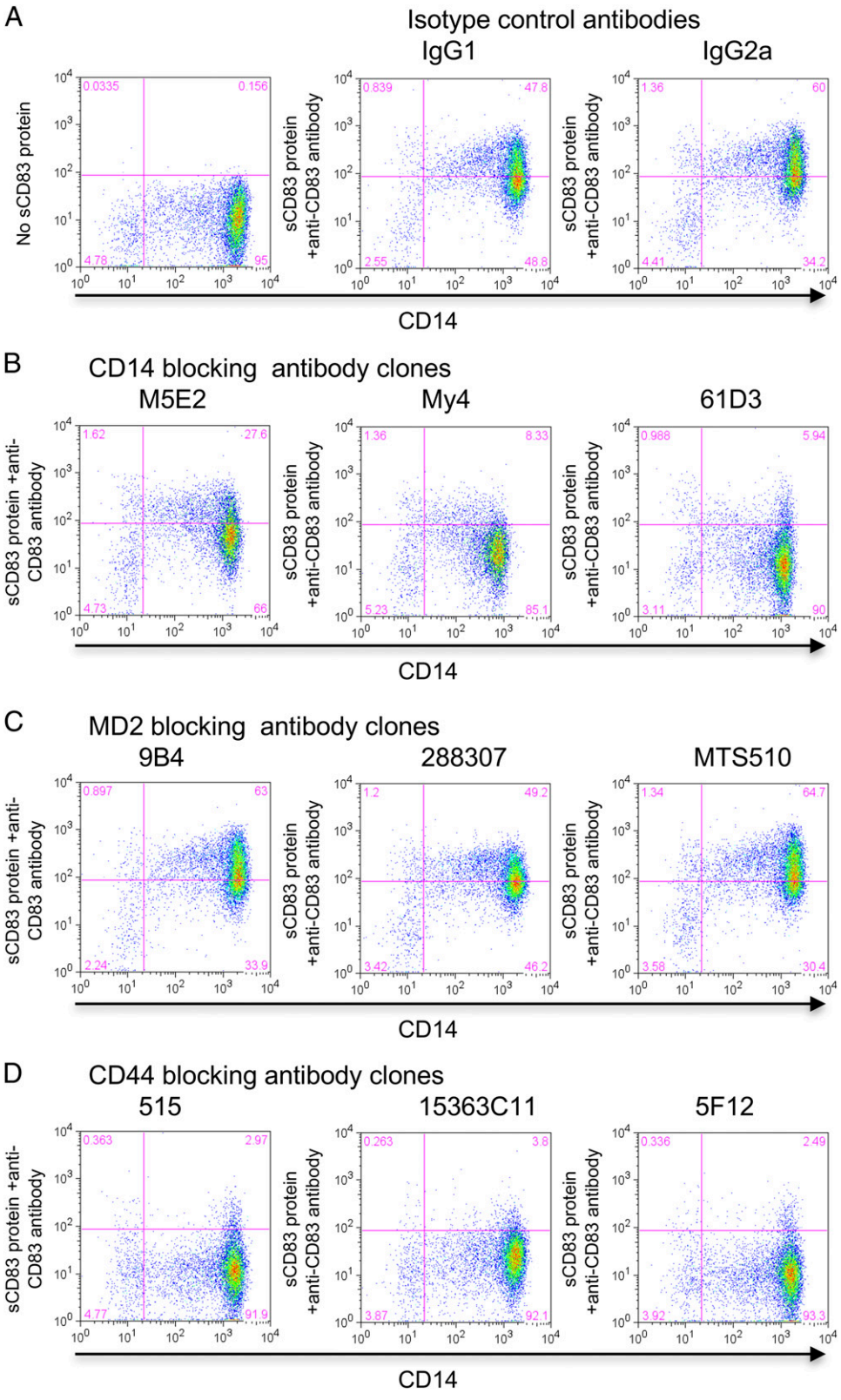

FIGURE 4. Blocking sCD83 binding in the presence of Abs to CD14, MD-2, TLR4, and CD44. (**A**) sCD83 binding was determined on CD14$^+$ monocytes, as described in *Materials and Methods*, in the presence of two isotype-control IgG Abs (middle and right panels). Background staining with the anti-CD83 Ab in the absence of sCD83 protein on CD14$^+$ monocytes (left panel). CD14 surface expression was measured using FITC-conjugated anti-CD14 Ab (clone MY4) that was added postwashing to blocked samples. (**B**) Anti-CD14 Ab clones M5E2 (left panel), My4 (middle panel), and 61D3 (right panel) were incubated with PBMCs prior to the addition of sCD83 protein, and sCD83 binding was measured on CD14$^+$ monocytes stained with FITC–anti-CD14 Ab. (**C**) Anti–MD-2 Ab clones 9B4 (left panel) and 288307 (middle panel) and anti–TLR4/MD-2 Ab clone MTS510 (right panel) were incubated with PBMCs prior to the addition of sCD83 protein, and sCD83 binding was measured on CD14$^+$ monocytes stained with FITC–anti-CD14 Ab. (**D**) Anti-CD44s Ab clones 515 (left panel), 15363C11 (middle panel), and 5F12 (right panel) were incubated with PBMCs prior to the addition of sCD83 protein, and sCD83 binding was measured on CD14$^+$ monocytes stained with FITC–anti-CD14 Ab. Data shown are representative of three experiments.

surface (Fig. 2C). By plotting the MFI values for bound sCD83 protein versus the MFI values of CD14, TLR4, CD44v6, or MD-2 surface expression, a statistically significant correlation was noted between the MFI values of bound sCD83 and cell surface expression of CD44v6 (Fig. 2Ciii) and MD-2 (Fig. 2Civ). No correlation was found between the MFI of bound sCD83 and MFI values for surface expression of CD14 (Fig. 2Ci) or TLR4 (Fig. 2Cii). Further binding analysis using PBMCs from a donor whose monocytes bound low levels of sCD83 (15.6%, Fig. 3A, left panel) showed that, if PBMCs were first treated with GM-CSF overnight, there was an increase in sCD83 binding (69.4%, Fig. 3A, right panel); a concurrent upregulation of CD44v6 expression from 39.6% (Fig. 3B, left panel) to 83.8% (Fig. 3B, right panel) was observed, and there was little change in MD-2 expression (Fig. 3C).

CD44 containing the v6 variant is essential for sCD83 binding

Given the observation that sCD83-binding cells are CD14, MD-2, TLR4, and CD44v6 positive, and all four molecules associate with the TLR4 heterodimer (37), we investigated which molecules in the TLR4/MD-2/CD14–CD44 complex were necessary or essential for the binding of sCD83 to the surface of monocytes. Ab-blocking experiments were used to determine which molecules are required for sCD83 binding to the cell surface of monocytes. sCD83 bound to 47.8 and 60% of $CD14^+$ monocytes in the presence of two isotype-control Abs (Fig. 4A, middle and right panels). Background staining in the absence of sCD83 protein is shown (Fig. 4A, left panel). Preincubation of monocytes with anti-CD14 Ab clone M5E2 reduced sCD83 binding to 27.6% (Fig. 4B, left panel), and clones My4 and 61D3 reduced sCD83 binding to 8.3% (Fig. 4B, middle panel) and 5.9% (Fig. 4, right panel), respectively. Interestingly, all three Ab clones can detect surface expression of CD14, but clone M5E2 reportedly is unable to block LPS-induced activation of monocytes (56). Because this clone showed less of a reduction in sCD83 binding, it suggests that sCD83 interacts with a region associated with LPS binding. We next evaluated the ability of anti–MD-2 Abs to reduce sCD83 surface binding (Fig. 4C). Only one of the two MD-2–specific Abs tested (clone 288307) partially reduced sCD83 binding to 49.2% (Fig. 4C, middle panel) versus 63% for clone 9B4 (Fig. 4C, left panel). Furthermore, the Ab clone MTS510, with specificity for the complexed TLR4/MD-2 molecules, did not reduce CD83 binding (64.7%) (Fig. 4C, right panel). Next, we investigated the contribution of CD44R to the ability of cells to bind sCD83 because CD44 was reported to associate with the TLR4 complex (47). As other investigators reported, CD44 recognition of hyaluronan regulates TLR4 inflammatory signals during acute pulmonary inflammation (44). These data, taken together with our preliminary observation that expression of CD44v6 is associated with sCD83 binding, led us to investigate the binding of sCD83 in the presence of Abs that target the standard extracellular region of CD44 (Fig. 4D). All three anti-CD44 Ab clones with specificity for the standard extracellular region of CD44 completely reduced sCD83 binding to the surface of monocytes, with residual sCD83 binding of 3–5% (Fig. 4D). In a separate experiment, sCD83 bound to 86.9% of $CD14^+$ cells (Fig. 5A, first panel), and anti-CD44 Ab reduced the binding to 10% of cells (Fig. 5A, second panel). However, if sCD83 protein was premixed with soluble recombinant MD-2 protein prior to the addition to cells, presumably to allow the sCD83/MD-2 complex to form, cell surface binding was partially restored from 10% (Fig. 5A, second panel) to 55.5% (Fig. 5A, fourth panel) in the presence of anti-CD44 blocking Ab. In the absence of anti-CD44 Ab, preincubation of sCD83 and MD-2 protein did not alter sCD83 cell surface binding (Fig. 5A, third panel). Additionally, if an Ab with specificity for the CD44v6 region, which recognizes an epitope along the stem region of the receptor, is added prior to the addition of sCD83 protein, no reduction in sCD83-bound protein is observed. The percentage of bound sCD83 protein was 93% in the absence of anti-CD44v6 Ab (Fig. 5B, open graph) and 89% in the presence of Ab (Fig 5B, shaded graph). Because all CD44Rs express the standard extracellular region but exhibit variation with regard to the variant regions present in the stem loop, we conclude that the extracellular domain of CD44 is necessary for sCD83 binding, and expression of at least the variant 6 region is required to facilitate sCD83 binding. Furthermore, increased abundance of MD-2 protein can overcome anti-CD44 Ab inhibition of sCD83 binding.

sCD83 binds to MD-2 with high affinity

Given the observation that the binding of sCD83 to monocytes was blocked with Abs to CD14 or CD44, and the addition of soluble MD-2 mediates CD44-independent sCD83 binding to the cell surface of monocytes, it was of interest to determine the binding affinities between sCD83 and the coreceptors CD14, CD44, and MD-2. To quantitate the binding of sCD83 to MD-2, CD44, and CD14, a cell-free ELISA-based assay was developed. Increasing concentrations of recombinant MD-2, CD44s, or CD14 protein were added to immobilized sCD83 protein, and the binding affinities were determined. MD-2 protein bound to sCD83 with a kDa of 7.2 nM; however, neither CD14 nor CD44s bound to sCD83 protein with a measurable affinity (Fig. 6A). The fact that the

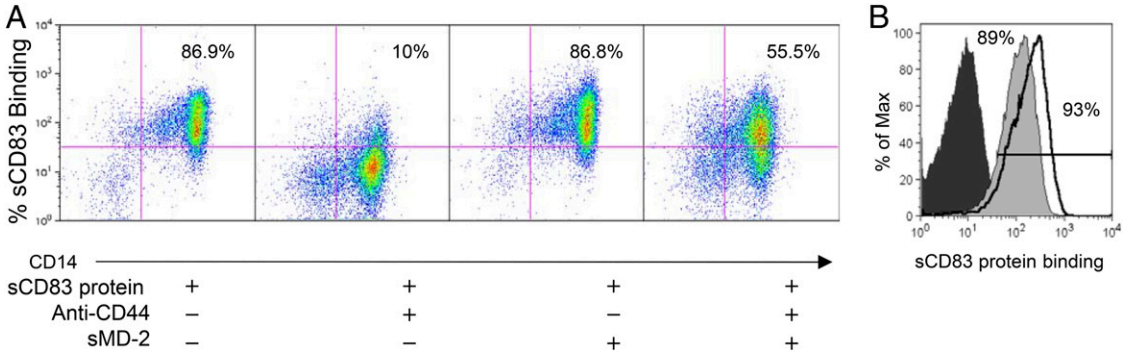

FIGURE 5. MD-2 enhances sCD83 binding to monocytes. (**A**) Percentage of bound sCD83 protein to $CD14^+$ cells in the absence of anti-CD44s (standard form) Ab and MD-2 protein (first panel). The percentage of sCD83 protein binding was determined in the presence of anti-CD44s Ab (clone IM-7, second panel) or with anti-CD44s Ab + soluble MD-2 protein (fourth panel). Cells were incubated with anti-CD44 Ab and then with sCD83 and MD-2 proteins premixed prior to addition to cells. The percentage of sCD83 binding in the presence of MD-2 protein without anti-CD44s Ab is shown (third panel). (**B**) sCD83 binding (shaded graph) on the cell surface in the presence of anti-CD44v6 Ab (clone VFF-7) or in the absence of anti-CD44v6 Ab (open graph). The filled graph shows staining with anti-CD83 Ab in the absence of sCD83 protein. Data shown are representative of two independent experiments.

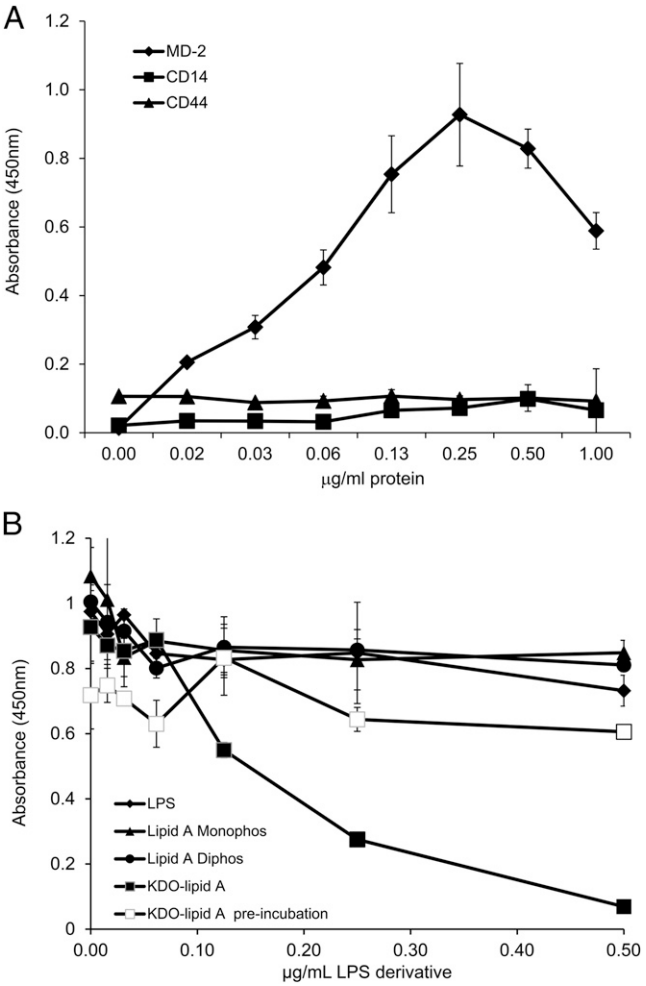

FIGURE 6. sCD83 binds to MD-2 with high affinity near the KDO–lipid A binding site on TLR4/MD-2. (**A**) Recombinant MD-2, CD14, or CD44 proteins were added to sCD83-coated plates at the indicated concentrations, and bound protein was detected using biotin-conjugated Abs to MD-2, CD14, or CD44, respectively. Nonspecific binding determined using plates not coated with sCD83 was subtracted from specific binding detection. (**B**) MD-2 protein (0.25 μg/ml) was coincubated with serial dilutions of LPS, KDO–lipid A, lipid A diphosphate, or lipid A monophosphate prior to addition to sCD83-coated plates. Alternatively, serial dilutions of KDO–lipid A were added to the sCD83-coated plates, and plates were washed prior to the addition of MD-2 protein. Biotinylated anti–MD-2 Ab was used to detect MD-2 protein bound to immobilized sCD83. Binding affinity for MD-2 was calculated using five-parameter logistic curve fitting within SigmaPlot software. Data shown are representative of two independent experiments.

binding assay with CD44s or CD14 protein did not yield a saturation curve suggests that sCD83 does not bind directly to CD44s or CD14. The crystal structure of agonist and antagonist ligands binding to the TLR4/MD-2 complex was determined (31). LPS-derived antagonists were tested as potential therapeutic candidates to treat sepsis by preventing signaling through the TLR4/MD-2 coreceptors (38). Therefore, it was of interest to test the ability of MD-2 protein to bind immobilized sCD83 protein in the presence of exogenous LPS or LPS derivatives KDO–lipid A, monophosphoryl–lipid A, and diphosphoryl–lipid A to map the sCD83 binding site on MD-2. Recombinant MD-2 protein was incubated with each of these LPS derivatives prior to addition to plates coated with sCD83 protein (Fig. 6B); if MD-2 bound to LPS, or the LPS derivatives blocked sCD83 binding, the interaction of sCD83 with MD-2 may mimic antagonist regulation of TLR signaling. Only the KDO–lipid A variant (■) preincubated with MD-2 prevented MD-2 binding to sCD83 (Fig. 6B). Neither Lipid A derivative containing one or two phosphate groups nor LPS preincubated with MD-2 protein blocked MD-2 binding to sCD83. However, if the KDO–lipid A variant was added to sCD83-bound plates and washed prior to the addition of MD-2 protein (□), it no longer blocked MD-2 binding to sCD83. This suggests that sCD83 does not directly bind LPS, and LPS preformed with MD-2 prevents sCD83 interaction with the TLR4/MD-2 complex. These data imply that sCD83 binds to MD-2 at a site close to the interaction of the KDO portion of the lipid molecule but distal to the lipid A tail. Moreover, the ability of anti-CD44s and anti-CD14 Abs to block sCD83 cell surface binding is related to the close proximity of these receptors to TLR4. MD-2 binding to sCD83 is reminiscent of its role in the transfer of LPS from CD14R to TLR4 leading to conformational changes and the initiation of signaling events. Taken together, these data indicate that the complex formed between MD-2 and sCD83 is stable, and MD-2 is the dominant high-affinity binding partner for sCD83.

sCD83 binding alters the TLR4/MD-2 signaling cascade at the level of IRAK-1 protein expression

Modulation of IRAKs is pivotal in regulating signals through the TLR4 complex (50, 57). Specifically, IRAK-1 is involved in the early signaling cascade downstream of MyD88, leading to induction of NF-κB and cytokine gene transcription (40). Interestingly, it was reported that CD44 can regulate TLR signaling by inducing the negative IRAK regulator IRAK-M (48), and tumor-derived hyaluronan interacts with CD44 and inhibits IRAK-1 expression in monocytes, leading to increases in IL-10 (58). Therefore, it was of interest to test the hypothesis that sCD83 signals through TLR4 and alters this cascade. We investigated the expression of IRAK proteins in the presence of sCD83 by purifying monocytes by negative selection and culturing them overnight in medium containing GM-CSF to induce expression of IRAK-1 protein, because freshly isolated monocytes do not express IRAK-1 protein, even when cultured in medium alone (data not shown). GM-CSF–cultured monocytes were incubated with sCD83 or LPS and assayed for the presence of IRAK-1, IRAK-2, IRAK-M, and IRAK-4 proteins (Fig. 7). IRAK-1 protein was detected in untreated cultures and LPS-treated cultures in contrast to cultures treated with sCD83 (Fig. 7A). Furthermore, no change in IRAK-2, IRAK-4, and IRAK-M protein levels was detected when cells were treated with sCD83 for 60 min (Fig. 7A). Given the loss of IRAK-1 protein expression within 60 min of treating cells with sCD83, we assessed IRAK-1 expression at earlier and later time points. IRAK-1 protein expression was lost rapidly by 10–15 min after sCD83 addition, in contrast to stimulation with LPS (Fig. 7B). This lack of IRAK-1 protein was sustained out past 2–3 d (Fig. 7C), and no evidence of protein restoration could be detected out to 7 d post-sCD83 addition (Fig. 7C, 7D). As shown with the early time course, no loss of IRAK-2, IRAK-M, or IRAK-4 was seen at 2–3 and 7 d post-sCD83 treatment (Fig. 7C, 7D). Interestingly, we did not detect any impact on downstream TRAF6 protein levels during the time course of IRAK-1 loss at 30 min or out to 6 and 24 h post-sCD83 treatment (Fig. 7E).

sCD83 suppresses T cell proliferation and induces IL-2 unresponsiveness

We next tested the functional immune-modulatory impact that sCD83 has on T cell proliferation. sCD83 was added to anti-CD3/anti-CD28–stimulated PBMCs containing monocytes. The addition of soluble T cell–specific stimulatory Abs allows APCs present in T cell cultures to cross-link TCRs and costimulatory

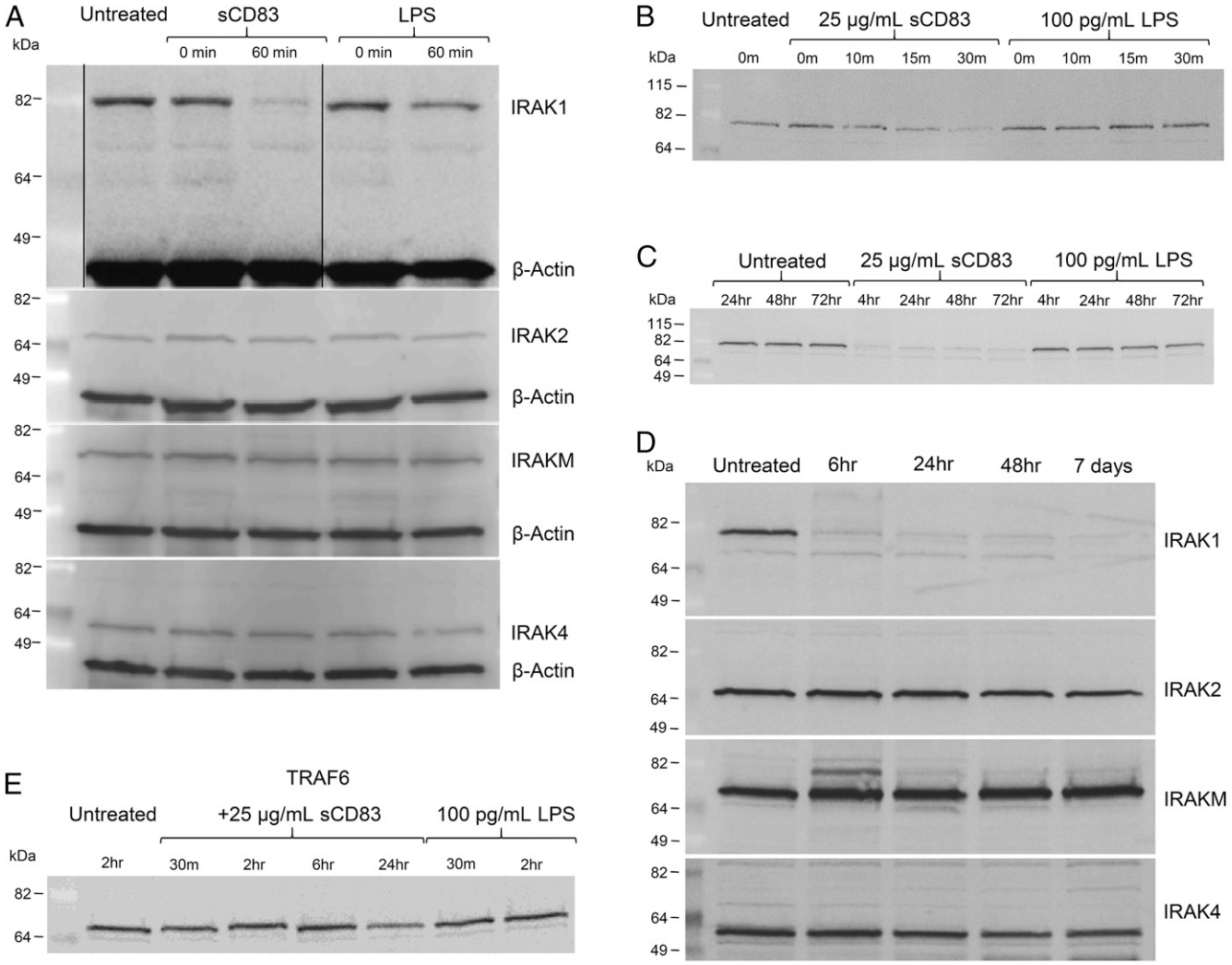

FIGURE 7. sCD83 signals through the TLR4/MD-2 coreceptor by downregulating IRAK-1 expression. Purified monocytes were cultured overnight in medium containing GM-CSF and then stimulated with 25 μg/ml sCD83 protein or 100 ng/ml LPS for 60 min (**A**), 10, 15, or 30 min (**B**), 24, 48, or 72 h (**C**), 6, 24, or 48 h and 7 d (**D**), or 30 min or 2 or 6 h (**E**). Cell lysates were prepared, and equivalent cellular protein concentrations were Western blotted with Abs to IRAK-1, IRAK-2, IRAK-M, IRAK-4, and TRAF6 or with β-actin as a loading control. Data shown are representative of three independent experiments.

molecules on the T cell, leading to T cell activation and proliferation. CFSE-labeled PBMCs from normal donors were stimulated in the presence of sCD83 for 6 d, and the percentage of proliferating $CD4^+$ T cells and $CD8^+$ T cells was measured by CFSE dilution. Representative dot plots show that sCD83 decreased the percentage of $CD4^+$ T cell proliferation (Fig. 8A, upper panels) and $CD8^+$ T cell proliferation (Fig. 8A, lower panels). Across a cohort of five donors tested, addition of sCD83 caused a statistically significant decrease in CD4 T cell proliferation (from 89 to 25%) and CD8 T cell proliferation (from 87 to 38%) (Fig. 8B). This prompted us to quantitate the absolute numbers of proliferating $CD4^+$ and $CD8^+$ T cells in the cultures treated with sCD83. sCD83 suppression of T cell proliferation was dose dependent; cultures treated with sCD83 had fewer total numbers of proliferating $CD4^+$ and $CD8^+$ T cells than did the untreated cultures (Fig. 8C). To assess the expansion of sCD83-treated $CD4^+$ and $CD8^+$ T cells upon secondary stimulation, IL-2 was added to previously stimulated cultures on day 8. Two days later, proliferation was measured by CFSE dilution over multiple cell divisions; zero cell divisions represents nonproliferating cells, and the number of proliferating $CD4^+$ or $CD8^+$ T cells per milliliter was determined for each subsequent cell division. $CD4^+$ and $CD8^+$ T cells stimulated previously in the presence of sCD83 were unable to respond to IL-2 addition compared with T cells stimulated previously in the absence of sCD83 (Fig. 8D). This suggests that sCD83 inhibits T cell proliferation when APCs are present and renders T cells unresponsive to further stimulation with IL-2.

Given that sCD83 binds to the MD-2 coreceptor of the TLR4 complex expressed on monocytes, and sCD83 addition to T cell cultures containing monocytes results in suppression of T cell proliferation, it was of interest to see whether LPS or KDO–lipid A would have a similar effect, because these molecules signal through TLR4 and may block T cell activation. Furthermore, recombinant sCD83 protein was derived from bacterial sources and could contain low levels of bacterial components, such as LPS, which could modulate T cell activation. T cell proliferation was determined in the presence of 50 μg/ml sCD83 or a combination of 100 ng/ml LPS and KDO–lipid A. Although sCD83 suppressed $CD4^+$ and $CD8^+$ T cell proliferation, the combination of LPS and KDO–lipid A did not block $CD4^+$ (Fig. 8E) or $CD8^+$ (Fig. 8F) T cell proliferation. Therefore, sCD83 inhibition of T cell proliferation functions through a different mechanism

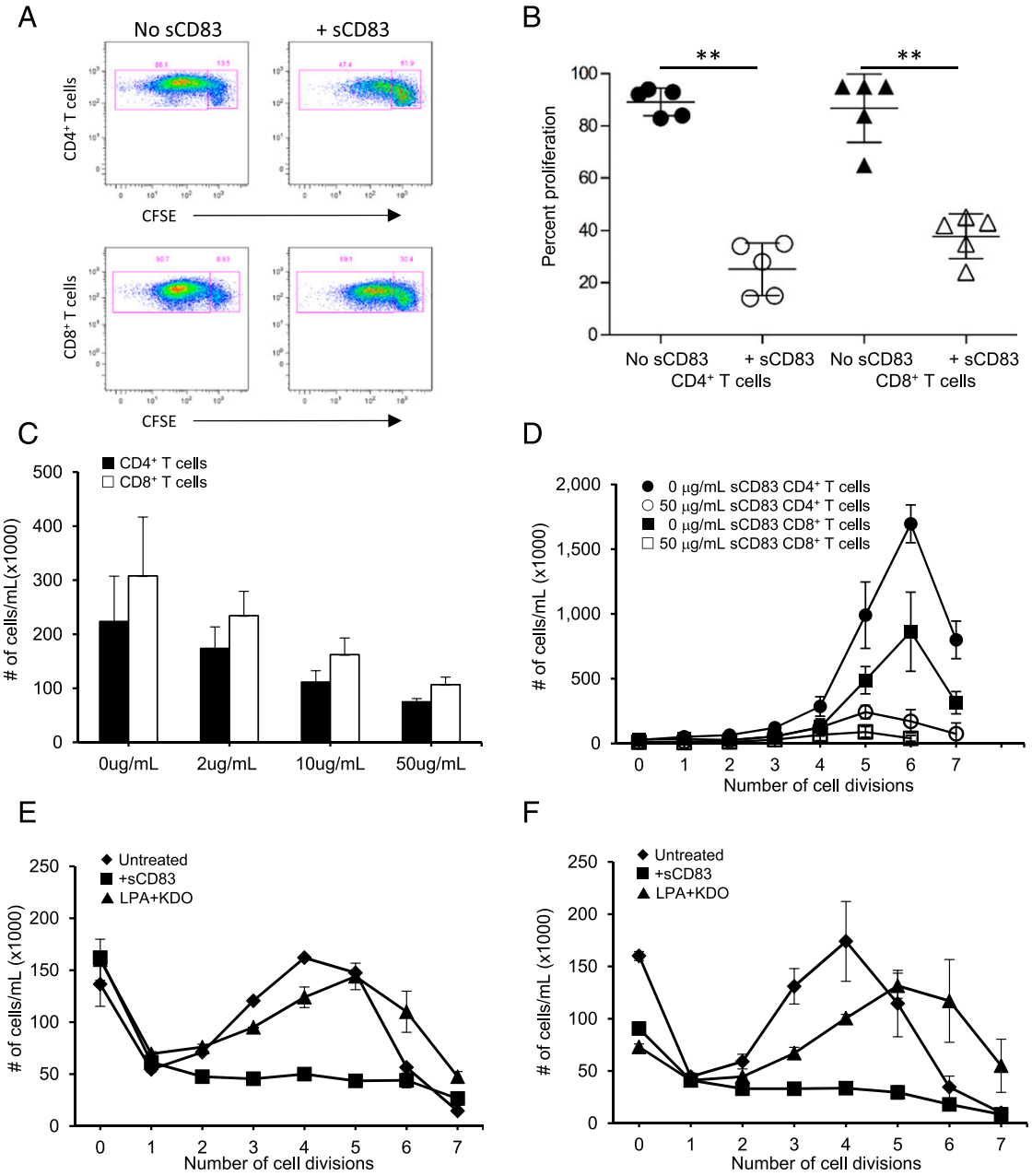

FIGURE 8. sCD83 blocks T cell proliferation and renders T cells unresponsive to IL-2. CFSE-labeled PBMCs were stimulated with anti-CD3 and anti-CD28 Abs for 6 d, with or without the addition of sCD83 protein. Proliferation was measured by CFSE dilution by flow cytometry. (**A**) Dot plots show the inhibition of proliferation by sCD83. The $CFSE^{low}$ gate shows $CD4^+$ or $CD8^+$ T cells that proliferated in the presence or absence of sCD83 protein, whereas the $CFSE^{high}$ gate shows nonproliferating cells. (**B**) Whisker plots showing the range of inhibition of sCD83 for five individual donors. Each point represents one donor. Cells were treated or not with sCD83, and the percentage of proliferation was measured on day 6 in untreated $CD4^+$ T cells (●), sCD83-treated $CD4^+$ T cells (○), untreated $CD8^+$ T cells (▲), and sCD83-treated $CD8^+$ T cells (△). (**C**) Cells were treated with 0, 2, 10, or 50 μg/ml sCD83, and the total number of proliferating $CD4^+$ T cells and $CD8^+$ T cells was calculated. (**D**) Eight days post–T cell stimulation, 20 U/ml IL-2 was added to PBMC cultures previously stimulated with anti-CD3/anti-CD28 Abs in the presence (○, □) or absence (●, ■) of sCD83 protein. Proliferation by CFSE dilution was determined 3 d later by measuring the number of $CD4^+$ T cells (○, ●) and $CD8^+$ T cells (□, ■) proliferating within each division. CFSE-treated human PBMCs were stimulated to proliferate with anti-CD3 and anti-CD28 Abs in the absence (♦) or presence of 50 μg/ml sCD83 (■) or 100 ng/ml LPS+KDO (▲), and the number of $CD4^+$ T cells (**E**) or $CD8^+$ T cells (**F**) proliferating within each division was determined 6 d later. All data points were run as replicates; error bars represent the range of each individual data point. Data sets are representative of two to five experiments from up to five individual donors. $^{**}p < 0.01$.

than LPS signaling, and sCD83 inhibition is independent of LPS contaminants.

sCD83 mechanism of action is mediated through COX-2 and IL-10 pathways, a potential role for IDO

Previous investigations of sCD83 preparations used to suppress T cell proliferation revealed that PGE_2, through COX-2 activation, was responsible for the ability of sCD83 to block T cell proliferation (28). We confirm those findings in this study and provide new evidence for a role for IL-10 and IDO in sCD83-dependent suppression of T cell cytokine secretion. sCD83 treatment resulted in suppression of IL-2 (Fig. 9A), IFN-γ (Fig. 9B), IL-5 (Fig. 9C), and IL-13 (Fig. 9D) secretion in stimulated cultures. Concurrently, there was an induction of IL-6 (Fig. 9E), IL-10 (Fig. 9F), and

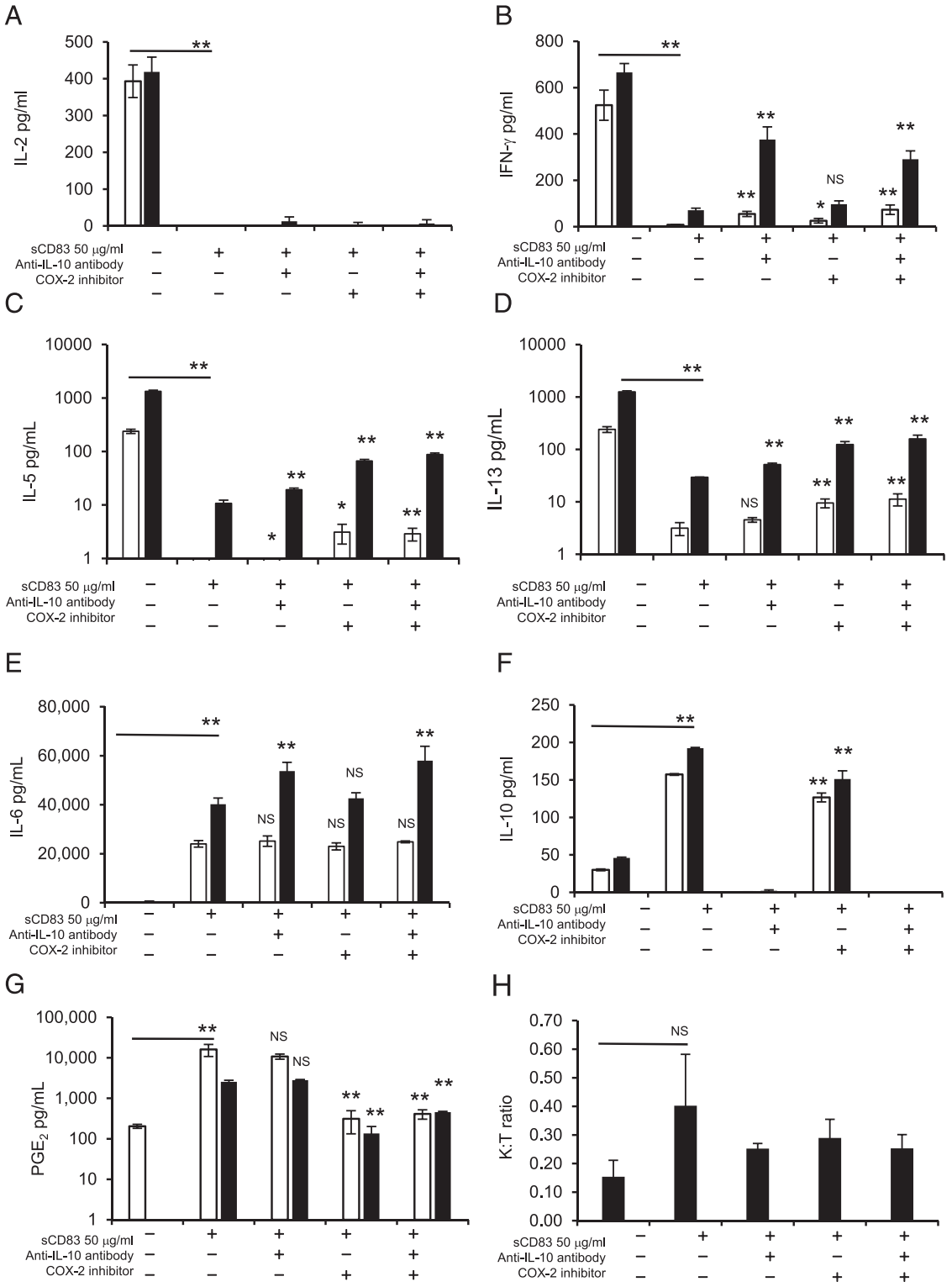

FIGURE 9. sCD83 modulates cytokine and PGE_2 secretion and induces IDO activity. Culture supernatant was collected 24 h (IL-2, IFN-γ, IL-6, IL-10, and PGE_2) or 4 d (IL-5 and IL-13) after PBMCs were stimulated with anti-CD3 and anti-CD28 Abs in the presence of sCD83 alone or in combination with anti–IL-10 Ab or the COX-2 inhibitor NS-398. Cytokine concentrations were determined by cytokine bead arrays for IL-2 (**A**), IFN-γ (**B**), IL-5 (**C**), IL-13 (**D**), IL-6 (**E**), and IL-10 (**F**). (**G**) PGE_2 concentration was determined using a competitive ELISA. (**H**) IDO activity was measured in 24-h culture supernatant from PBMCs that were stimulated to proliferate with anti-CD3 and anti-CD28 Abs. Some cultures were left untreated or were treated with 50 μg/ml sCD83 in combination with anti–IL-10 Ab or COX-2 inhibitor. Error bars represent SD of cytokine bead array data sets. Data sets are representative of two to four experiments. Open bars, normal donor 1; closed bars, normal donor 2. Statistics shown above horizontal lines represent comparison of untreated samples with sCD83-treated samples. Statistics shown above individual bars represent comparison of sCD83-treated sample with samples treated in combination with anti–IL-10 Ab or the COX-2 inhibitor for each donor. $*p < 0.05$, $**p < 0.01$.

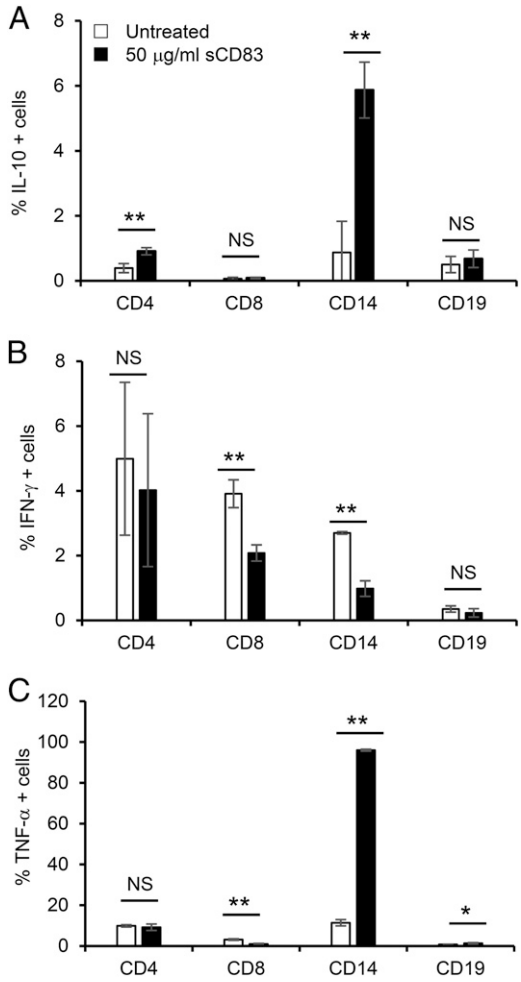

FIGURE 10. sCD83 induces IL-10 and TNF-α secretion from monocytes. Normal human PBMCs were stimulated with anti-CD3 and anti-CD28 Abs and treated or not with sCD83 for 24 h. Intracellular cytokine expression was measured by flow cytometry. (**A**) IL-10. (**B**) IFN-γ. (**C**) TNF-α. Data are representative of two normal donors and two separate experiments. $*p < 0.05$, $**p < 0.01$.

PGE_2 (Fig. 9G). Partial reversal of sCD83-dependent inhibition of IFN-γ is dependent on neutralization of IL-10 (Fig. 9B), and blocking PGE_2 secretion with a COX-2 inhibitor partially restored IL-5 (Fig. 9C) and IL-13 (Fig. 9D) in both donors tested. The COX-2 inhibitor blocked PGE_2 production (Fig. 9G), as previously reported (28), and, in our experiments, the COX-2 inhibitor partially suppressed sCD83-induced IL-10 secretion (Fig. 9F), with minimal effect on IL-6 (Fig. 9E). The predominant cell type secreting IL-10 in the sCD83-treated cultures was $CD14^+$ monocytes, with a small contribution by $CD4^+$ T cells. No difference in IL-10 secretion by $CD8^+$ T cells and $CD19^+$ B cells was detected (Fig. 10A). Furthermore, inhibition of IFN-γ secretion by $CD8^+$ T cells and $CD14^+$ monocytes in the cultures is more sensitive to sCD83 than is that by $CD4^+$ T cells (Fig. 10B). Interestingly, we observed a strong induction of TNF-α by $CD14^+$ monocytes in the sCD83-treated cultures, with no impact on TNF-α secretion by $CD4^+$ T cells and a decrease in TNF-α secretion by $CD8^+$ T cells (Fig. 10C). These data suggest differential regulation of these cytokines post–TLR4/MD-2 engagement with sCD83. It was reported that IL-10 secretion can be upregulated in a COX-2–dependent manner through feedback regulation of PGE_2 (59, 60). This positions PGE_2 upstream in the sCD83 signaling cascade of anti-inflammatory modulators leading to IL-10 induction. Interestingly, we observed inhibition of IFN-γ secretion that prompted us to investigate a link between IDO activity and IFN-γ (61, 62). We measured IDO enzyme activity in PBMC cultures stimulated in the presence of sCD83. IDO activity was increased in sCD83-treated cultures, shown as an increase in the kynurenine/tryptophan ratio (Fig. 9H). However, this increase was not statistically significant. Regardless, this induction of IDO activity could be partially blocked in the presence of the COX-2 inhibitor (Fig. 9H), whereas blocking IL-10 had little or no effect. Therefore, sCD83-induced suppression of T cell cytokine profiles is mediated through the TLR4/MD-2 coreceptor, and it results in the induction of a combination of PGE_2, IDO, IL-10, and TNF-α. These data are consistent with our previous observation that sCD83-mediated corneal allograft survival and long-term kidney allograft survival were abolished in the presence of the IDO-specific inhibitor 1 methyl-tryptophan (20, 27).

Discussion

CD83 plays a central role in regulating the immune system and is a prime target for therapeutic intervention. Various preparations of recombinant sCD83 were reported to modulate immune responses; however, until now, the sCD83 receptor/ligand on the appropriate target cell has not been identified. Recently, it was suggested that CD83 may act in a homotypic way (30); however, the investigators failed to demonstrate a clear biophysical interaction and, therefore, the exact receptor for sCD83 on cells has yet to be determined. Other investigators showed that sCD83 binds to human monocytes (28). We confirmed the binding of sCD83 to monocytes in this study and extended the APC types binding sCD83 to include $CD14^+$ plasmacytoid and myeloid DC subsets present in peripheral blood. The presence of $CD14^+$ blood DCs was originally reported and shown to identify a precursor DC population that was capable of stimulating T cell responses (63). This raises the possibility that binding of sCD83 to $CD14^+$ blood DCs may influence DC maturation and impact T cell stimulation. Furthermore, we identified a small population of $CD19^+/CD14^-$ B cells that bound sCD83 protein. More importantly, we provide, for the first time to our knowledge, direct evidence that sCD83 binds to the MD-2 molecule, the coreceptor for TLR4 expressed on human monocytes. Identification of the MD-2 coreceptor as the high-affinity binding partner for sCD83 allowed us to map early signals delivered through sCD83 engagement of TLR4/MD-2 that result in secretion of PGE_2, IL-10. These anti-inflammatory mediators are responsible for the ability of sCD83 to block T cell activation and contribute to the overall suppression of proliferation and secretion of IL-2, IL-5, IL-13, and INF-γ. Moreover, prior exposure to sCD83 induces a state of T cell anergy that is defined by a lack of subsequent proliferation upon exposure to IL-2.

Our initial characterization of sCD83 binding to monocytes revealed a contribution of other coreceptors that are involved in coordinating TLR4 signaling. Abs directed to CD14 and the standard extracellular domain of CD44 expressed on all variants blocked sCD83 binding, revealing a close proximity of CD14 and CD44 with the sCD83-TLR4/MD-2 receptor complex. However, neither the recombinant CD14 nor CD44s protein bound with high affinity to sCD83 under cell-free conditions that facilitate direct protein–protein interactions, but sCD83 bound with high affinity to recombinant MD-2 protein under the same conditions. Therefore, the docking protein within the CD14/TLR4/MD-2–CD44v6 complex is the MD-2 molecule. CD44s containing the standard extracellular domain can be expressed on the cell surface in multiple forms, depending on the expression of variant regions of the stem region (v1–v10) (49). During our screening for sCD83 binding to monocytes, we discovered that the level of MD-2 and

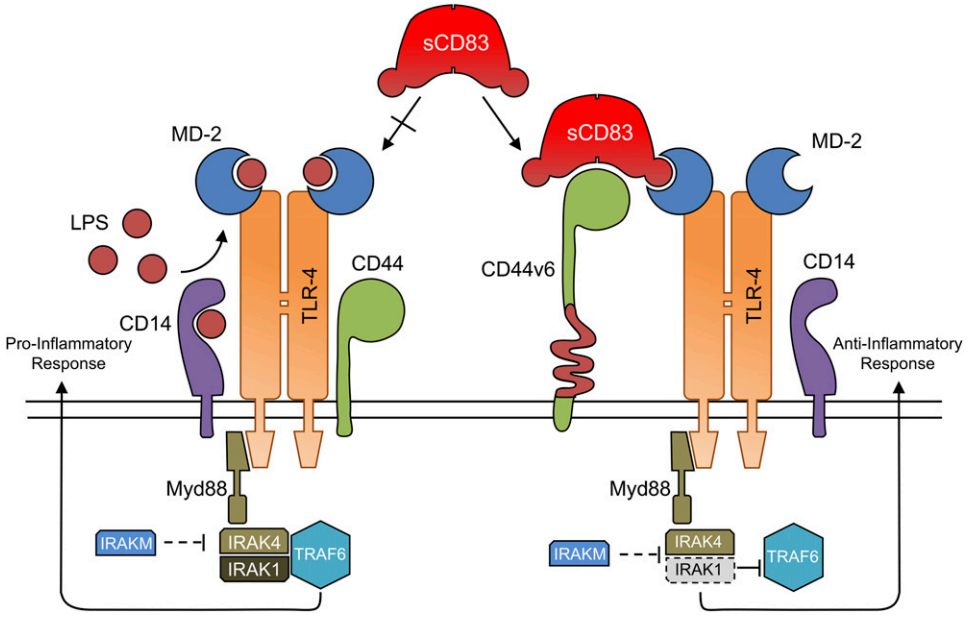

FIGURE 11. Schematic model depicting the interaction of sCD83 protein with the TLR4/MD-2 complex. TLR4 proinflammatory signals originate after LPS is bound through the interaction with CD14 and MD-2. MD-2 binding to LPS induces a conformational change in the MD-2/TLR4 heterodimers allowing the transduction of signals through the IRAK family of tyrosine kinases. sCD83 binds directly to MD-2 within the MD-2/TLR4 complex facilitated by CD44v6. The results of Ab-blocking experiments provide a role for the association of CD14 and CD44v6 within close proximity to the sCD83 binding site on the TLR4/MD-2 complex. sCD83 binding through TLR4/MD-2 results in a rapid and sustained loss of IRAK-1 leading to an altered signaling cascade toward an anti-inflammatory response.

CD44v6 surface expression can vary and impact the binding of sCD83 protein. By comparing the cell surface expression level of MD-2 or CD44v6 with the relative amounts of sCD83 bound to the cell surface, a correlation was observed that linked the expression levels of MD-2 or CD44v6 with sCD83 surface binding. Furthermore, if sCD83 binding was low, higher levels of binding could be restored if monocytes were stimulated with GM-CSF to upregulate CD44v6 protein expression. Moreover, if MD-2 protein was first bound to sCD83 in solution, sCD83 binding could be restored in the presence of Abs to CD44 that normally block sCD83 binding, suggesting that MD-2 tethers sCD83 into the TLR4 complex, and CD44 is in close proximity to the complex. Because we could not show a direct protein–protein interaction between CD44s and sCD83, but Abs directed to the CD44s portion of CD44R blocked binding, we propose a model (Fig. 11) whereby sCD83 binding to monocytes is dependent on the expression of the CD44v6 variant that expresses the standard extracellular domain with at least the v6 variant of the stem loop region. The CD44v6 form of CD44 facilitates the conformation necessary to allow sCD83 to bind to MD-2 within the complex. The normal function of MD-2 is to tether LPS to TLR4, which leads to potent proinflammatory signals through heterodimerization of the receptor (31). Ligand engagement of TLR4/MD-2 dimers induces a signaling cascade downstream of MyD88 activation involving the phosphorylation of the adaptor protein IRAK-1 via IRAK-4. Activated IRAK-1 tethers to TRAF6 and leads to the nuclear translocation of NF-κB, inducing a proinflammatory cytokine cascade (40, 64, 65).

Downstream regulation of TLR4 signaling occurs at several checkpoints to modulate excessive inflammation, especially during resolution of inflammation (40, 41). Downregulation of IRAK-1 protein was reported in models of LPS tolerance (57), and loss of IRAK-1 is reported in tolerogenic DCs (66). The concept of antagonist ligands modulating TLR4 function was investigated in models of autoimmune arthritis (67), myocardial ischemia (68), and endotoxin-induced uveitis (69). Spontaneous models of colitis in mice using TLR4 knockouts revealed disease exacerbation that was dependent on TLR4 signals and IL-10 (70). One such pathway of TLR4 regulation is at a point of induction of IL-10 through a COX-2–dependent mechanism (71). In this article, we provide evidence, for the first time to our knowledge, that sCD83 engages the coreceptor MD-2 associated with TLR4 during early monocyte activation and results in sustained downregulation of IRAK-1. Whether it is through a loss of protein expression or protein degradation requires further studies to elucidate the exact mechanism modulating IRAK-1 levels by sCD83. In our model, a lack of IRAK-1 protein results in a shift to an anti-inflammatory state characterized by PGE_2 and IL-10 secretion. Additionally, sCD83 was shown to prevent experimental autoimmune encephalomyelitis (25) and colitis (26) in murine models, both of which were shown to be critically dependent on IRAK-1 activity (51, 72). Interestingly, we saw no evidence for upregulation of IRAK-M, the pseudokinase shown to be a negative regulator of TLR signaling (73). Although the exact signaling cascade through TLR4 that links COX-2 activation and IL-10 in our system is under investigation, other investigators showed a link between IL-10 production and COX-2 in non-small cell lung carcinoma patients (74). Furthermore, IL-10 was reported to upregulate MD-2 and CD14 (75), which may have the added effect of enhancing the tolerogenic properties of sCD83 by providing more coreceptors to interact with sCD83. The addition of a COX-2 inhibitor during T cell stimulation in the presence of sCD83 resulted in a decrease in PGE_2 and IL-10 secretion, whereas anti–IL-10 neutralizing Abs do not inhibit PGE_2 secretion. Therefore, we place sCD83-induced IL-10 secretion downstream of COX-2 activity. Upon further investigation of the sCD83 signaling pathway, we revealed a role for IDO in this pathway that was also dependent on COX-2. This suggests that sCD83 signals via tolerogenic pathways and generates IL-10 secretion and IDO in a COX-2/PGE_2–dependent mechanism. This anti-inflammatory phenotype is similar to what

was reported for myeloid-derived suppressor cells (76). We propose a model whereby sCD83 induces a positive-feedback loop based on early induction of PGE_2 that enhances COX-2 activation, leading to IL-10 secretion and IDO activity. This is reminiscent of the functional phenotype of immature DCs that, when exposed to PGE_2 during the early differentiation of DCs, leads to an anti-inflammatory phenotype expressing IL-10 and IDO (77). The specific cell type responsible for PGE_2 secretion and IDO activity remains to be determined, and further studies are warranted to help define their role in sCD83-mediated T cell suppression. Interestingly, we observed enhanced TNF-α secretion by $CD14^+$ monocytes in sCD83-treated cultures, which may have the additive effect of modulating IDO activity (78). Further investigation of the role of TNF-α in sCD83-mediated suppression is also warranted. Other investigators reported secretion of PGE_2, but not IL-10, when PBMCs are stimulated in the presence of a CD83–Ig fusion protein (28). The differences reported in the cytokine profile may be due to the differences in the preparations of sCD83. The sCD83–Ig fusion protein may not bind to the TLR4/MD-2 complex with sufficient affinity; therefore, it may transmit only a partial signal resulting in upstream signaling that leads to PGE_2 secretion but is insufficient to induce IL-10. The consequence of IL-10, TNF-α, and PGE_2 secretion coupled with IDO activity after sCD83 addition to T cell–stimulated cultures may lead to a block in T cell proliferation and a decrease in IL-2 secretion. Furthermore, T cells activated in the presence of sCD83 are unable to respond to further stimulation with exogenous IL-2. This is very similar to what is reported when T cells are stimulated in conditions containing IL-10 (79).

Previous studies showed that a short course of sCD83 administered to mice receiving orthotopic kidney allograft transplants resulted in graft survival > 100 d compared with a median survival of 35 d in untreated animals (19). To further understand the molecular basis for how sCD83 prevents allograft rejection, we tested the dependency of sCD83 activity on TLR4 signaling by using TLR4-deficient mice as kidney donors. Preliminary results provided evidence that, even with sCD83 administration to the recipient, the donor organ from TLR4-deficient animals was rejected at a median of 41.4 d, a similar time frame for animals not treated with sCD83. Therefore, we propose one possible mechanism in the transplant model: when sCD83 is administered to the recipient, the donor organ is no longer susceptible to the tolerogenic signals provided by sCD83 due to a lack of TLR4/MD-2. Therefore, there is no localized tolerance induced by sCD83-mediated secretion of IL-10, TNF-α, and PGE_2 at the organ site. Further experiments are required to provide definitive proof regarding this mechanism of tolerance. Therefore, sCD83 induces a state of long-term unresponsiveness similar to T cell anergy (80). This ability of sCD83 to render Ag-specific T cells unable to respond to continued stimuli would be an advantageous therapeutic agent to treat a variety of autoimmune diseases and prevent graft rejection.

Acknowledgments

We thank Bob Walker for help with preparation of the figures.

Disclosures

J.M.H., E.W.G., M.N., I.Y.T., C.A.N., and M.A.D. are full-time employees with Argos Therapeutics and hold stock options with the company. The other authors have no financial conflicts of interest.

References

1. Fujimoto, Y., and T. F. Tedder. 2006. CD83: a regulatory molecule of the immune system with great potential for therapeutic application. *J. Med. Dent. Sci.* 53: 85–91.
2. Hock, B. D., M. Kato, J. L. McKenzie, and D. N. Hart. 2001. A soluble form of CD83 is released from activated dendritic cells and B lymphocytes, and is detectable in normal human sera. *Int. Immunol.* 13: 959–967.
3. Prazma, C. M., and T. F. Tedder. 2008. Dendritic cell CD83: a therapeutic target or innocent bystander? *Immunol. Lett.* 115: 1–8.
4. Kreiser, S., J. Eckhardt, C. Kuhnt, M. Stein, L. Krzyzak, C. Seitz, C. Tucher, I. Knippertz, C. Becker, C. Gunther, A. Steinkasserer, and M. Lechmann. 2014. Murine CD83-positive T cells mediate suppressor functions in vitro and in vivo. *Immunobiology* 220: 270–279.
5. Prechtel, A. T., N. M. Turza, A. A. Theodoridis, and A. Steinkasserer. 2007. CD83 knockdown in monocyte-derived dendritic cells by small interfering RNA leads to a diminished T cell stimulation. *J. Immunol.* 178: 5454–5464.
6. Aerts-Toegaert, C., C. Heirman, S. Tuyaerts, J. Corthals, J. L. Aerts, A. Bonehill, K. Thielemans, and K. Breckpot. 2007. CD83 expression on dendritic cells and T cells: correlation with effective immune responses. *Eur. J. Immunol.* 37: 686–695.
7. Kruse, M., O. Rosorius, F. Krätzer, D. Bevec, C. Kuhnt, A. Steinkasserer, G. Schuler, and J. Hauber. 2000. Inhibition of CD83 cell surface expression during dendritic cell maturation by interference with nuclear export of CD83 mRNA. *J. Exp. Med.* 191: 1581–1590.
8. Kruse, M., O. Rosorius, F. Krätzer, G. Stelz, C. Kuhnt, G. Schuler, J. Hauber, and A. Steinkasserer. 2000. Mature dendritic cells infected with herpes simplex virus type 1 exhibit inhibited T-cell stimulatory capacity. *J. Virol.* 74: 7127–7136.
9. Dudziak, D., F. Nimmerjahn, G. W. Bornkamm, and G. Laux. 2005. Alternative splicing generates putative soluble CD83 proteins that inhibit T cell proliferation. *J. Immunol.* 174: 6672–6676.
10. Baleeiro, R. B., and J. A. Barbuto. 2008. Local secretion/shedding of tumor-derived CD83 molecules as a novel tumor escape mechanism. *Mol. Immunol.* 45: 3502–3504.
11. Hock, B. D., L. F. Haring, A. Steinkasserer, K. G. Taylor, W. N. Patton, and J. L. McKenzie. 2004. The soluble form of CD83 is present at elevated levels in a number of hematological malignancies. *Leuk. Res.* 28: 237–241.
12. Hock, B. D., L. J. Fernyhough, S. M. Gough, A. Steinkasserer, A. G. Cox, and J. L. McKenzie. 2009. Release and clinical significance of soluble CD83 in chronic lymphocytic leukemia. *Leuk. Res.* 33: 1089–1095.
13. Sénéchal, B., A. M. Boruchov, J. L. Reagan, D. N. Hart, and J. W. Young. 2004. Infection of mature monocyte-derived dendritic cells with human cytomegalovirus inhibits stimulation of T-cell proliferation via the release of soluble CD83. *Blood* 103: 4207–4215.
14. Lundell, A. C., K. Andersson, E. Josefsson, A. Steinkasserer, and A. Rudin. 2007. Soluble CD14 and CD83 from human neonatal antigen-presenting cells are inducible by commensal bacteria and suppress allergen-induced human neonatal Th2 differentiation. *Infect. Immun.* 75: 4097–4104.
15. Guo, Y., R. Li, X. Song, Y. Zhong, C. Wang, H. Jia, L. Wu, D. Wang, F. Fang, J. Ma, et al. 2014. The expression and characterization of functionally active soluble CD83 by *Pichia pastoris* using high-density fermentation. *PLoS One* 9: e89264.
16. Lechmann, M., E. Kremmer, H. Sticht, and A. Steinkasserer. 2002. Overexpression, purification, and biochemical characterization of the extracellular human CD83 domain and generation of monoclonal antibodies. *Protein Expr. Purif.* 24: 445–452.
17. Zhang, L., N. Narayanan, S. R. Brand, C. A. Nicolette, M. Baroja, J. Arp, H. Wang, M. Moo-Young, and C. P. Chou. 2010. Structural identification of recombinant human CD83 mutant variant as a potent therapeutic protein. *Protein Expr. Purif.* 73: 140–146.
18. Ge, W., J. Arp, D. Lian, W. Liu, M. L. Baroja, J. Jiang, S. Ramcharran, F. Z. Eldeen, E. Zinser, A. Steinkasserer, et al. 2010. Immunosuppression involving soluble CD83 induces tolerogenic dendritic cells that prevent cardiac allograft rejection. *Transplantation* 90: 1145–1156.
19. Lan, Z., D. Lian, W. Liu, J. Arp, B. Charlton, W. Ge, S. Brand, D. Healey, M. DeBenedette, C. Nicolette, et al. 2010. Prevention of chronic renal allograft rejection by soluble CD83. *Transplantation* 90: 1278–1285.
20. Lan, Z., W. Ge, J. Arp, J. Jiang, W. Liu, D. Gordon, D. Healey, M. DeBenedette, C. Nicolette, B. Garcia, and H. Wang. 2010. Induction of kidney allograft tolerance by soluble CD83 associated with prevalence of tolerogenic dendritic cells and indoleamine 2,3-dioxygenase. *Transplantation* 90: 1286–1293.
21. Xu, J. F., B. J. Huang, H. Yin, P. Xiong, W. Feng, Y. Xu, M. Fang, F. Zheng, C. Y. Wang, and F. L. Gong. 2007. A limited course of soluble CD83 delays acute cellular rejection of MHC-mismatched mouse skin allografts. *Transpl. Int.* 20: 266–276.
22. Lechmann, M., N. Kotzor, E. Zinser, A. T. Prechtel, H. Sticht, and A. Steinkasserer. 2005. CD83 is a dimer: comparative analysis of monomeric and dimeric isoforms. *Biochem. Biophys. Res. Commun.* 329: 132–139.
23. Staab, C., P. Mühl-Zürbes, A. Steinkasserer, and M. Kummer. 2010. Eukaryotic expression of functionally active recombinant soluble CD83 from HEK 293T cells. *Immunobiology* 215: 849–854.
24. Lechmann, M., D. J. Krooshoop, D. Dudziak, E. Kremmer, C. Kuhnt, C. G. Figdor, G. Schuler, and A. Steinkasserer. 2001. The extracellular domain of CD83 inhibits dendritic cell-mediated T cell stimulation and binds to a ligand on dendritic cells. *J. Exp. Med.* 194: 1813–1821.
25. Zinser, E., M. Lechmann, A. Golka, M. B. Lutz, and A. Steinkasserer. 2004. Prevention and treatment of experimental autoimmune encephalomyelitis by soluble CD83. *J. Exp. Med.* 200: 345–351.
26. Eckhardt, J., S. Kreiser, M. Döbbeler, C. Nicolette, M. A. DeBenedette, I. Y. Tcherepanova, C. Ostalecki, A. J. Pommer, C. Becker, C. Günther, et al. 2014. Soluble CD83 ameliorates experimental colitis in mice. *Mucosal Immunol.* 7: 1006–1018.
27. Bock, F., S. Rössner, J. Onderka, M. Lechmann, M. T. Pallotta, F. Fallarino, L. Boon, C. Nicolette, M. A. DeBenedette, I. Y. Tcherepanova, et al. 2013.

Topical application of soluble CD83 induces IDO-mediated immune modulation, increases Foxp3+ T cells, and prolongs allogeneic corneal graft survival. *J. Immunol.* 191: 1965–1975.
28. Chen, L., Y. Zhu, G. Zhang, C. Gao, W. Zhong, and X. Zhang. 2011. CD83-stimulated monocytes suppress T-cell immune responses through production of prostaglandin E2. *Proc. Natl. Acad. Sci. USA* 108: 18778–18783.
29. Scholler, N., M. Hayden-Ledbetter, K. E. Hellström, I. Hellström, and J. A. Ledbetter. 2001. CD83 is an I-type lectin adhesion receptor that binds monocytes and a subset of activated CD8+ T cells [corrected]. [Published erratum appears in 2009 *J. Immunol.* 182: 1772–1773.] *J. Immunol.* 166: 3865–3872.
30. Bates, J. M., K. Flanagan, L. Mo, N. Ota, J. Ding, S. Ho, S. Liu, M. Roose-Girma, S. Warming, and L. Diehl. 2015. Dendritic cell CD83 homotypic interactions regulate inflammation and promote mucosal homeostasis. *Mucosal Immunol.* 8: 414–428.
31. Park, B. S., D. H. Song, H. M. Kim, B. S. Choi, H. Lee, and J. O. Lee. 2009. The structural basis of lipopolysaccharide recognition by the TLR4–MD-2 complex. *Nature* 458: 1191–1195.
32. Takeda, K., and S. Akira. 2001. Regulation of innate immune responses by Toll-like receptors. *Jpn. J. Infect. Dis.* 54: 209–219.
33. Kirschning, C. J., and S. Bauer. 2001. Toll-like receptors: cellular signal transducers for exogenous molecular patterns causing immune responses. *Int. J. Med. Microbiol.* 291: 251–260.
34. Beutler, B. 2002. TLR4 as the mammalian endotoxin sensor. *Curr. Top. Microbiol. Immunol.* 270: 109–120.
35. Park, B. S., and J. O. Lee. 2013. Recognition of lipopolysaccharide pattern by TLR4 complexes. *Exp. Mol. Med.* 45: e66.
36. Triantafilou, M., K. Brandenburg, S. Kusumoto, K. Fukase, A. Mackie, U. Seydel, and K. Triantafilou. 2004. Combinational clustering of receptors following stimulation by bacterial products determines lipopolysaccharide responses. *Biochem. J.* 381: 527–536.
37. da Silva Correia, J., K. Soldau, U. Christen, P. S. Tobias, and R. J. Ulevitch. 2001. Lipopolysaccharide is in close proximity to each of the proteins in its membrane receptor complex. transfer from CD14 to TLR4 and MD-2. *J. Biol. Chem.* 276: 21129–21135.
38. Kim, H. M., B. S. Park, J. I. Kim, S. E. Kim, J. Lee, S. C. Oh, P. Enkhbayar, N. Matsushima, H. Lee, O. J. Yoo, and J. O. Lee. 2007. Crystal structure of the TLR4–MD-2 complex with bound endotoxin antagonist Eritoran. *Cell* 130: 906–917.
39. Bode, J. G., C. Ehlting, and D. Häussinger. 2012. The macrophage response towards LPS and its control through the p38(MAPK)-STAT3 axis. *Cell. Signal.* 24: 1185–1194.
40. Ringwood, L., and L. Li. 2008. The involvement of the interleukin-1 receptor-associated kinases (IRAKs) in cellular signaling networks controlling inflammation. *Cytokine* 42: 1–7.
41. O'Neill, L. A. 2008. When signaling pathways collide: positive and negative regulation of toll-like receptor signal transduction. *Immunity* 29: 12–20.
42. Jain, A., S. Kaczanowska, and E. Davila. 2014. IL-1 receptor-associated kinase signaling and its role in inflammation, cancer progression, and therapy resistance. *Front. Immunol.* 5: 553.
43. Bunt, S. K., V. K. Clements, E. M. Hanson, P. Sinha, and S. Ostrand-Rosenberg. 2009. Inflammation enhances myeloid-derived suppressor cell cross-talk by signaling through Toll-like receptor 4. *J. Leukoc. Biol.* 85: 996–1004.
44. Liang, J., D. Jiang, J. Griffith, S. Yu, J. Fan, X. Zhao, R. Bucala, and P. W. Noble. 2007. CD44 is a negative regulator of acute pulmonary inflammation and lipopolysaccharide-TLR signaling in mouse macrophages. *J. Immunol.* 178: 2469–2475.
45. del Fresno, C., L. Soler-Rangel, A. Soares-Schanoski, V. Gómez-Piña, M. C. González-León, L. Gómez-García, E. Mendoza-Barberá, A. Rodríguez-Rojas, F. García, P. Fuentes-Prior, et al. 2007. Inflammatory responses associated with acute coronary syndrome up-regulate IRAK-M and induce endotoxin tolerance in circulating monocytes. *J. Endotoxin Res.* 13: 39–52.
46. Shibolet, O., and D. K. Podolsky. 2007. TLRs in the Gut. IV. Negative regulation of Toll-like receptors and intestinal homeostasis: addition by subtraction. *Am. J. Physiol. Gastrointest. Liver Physiol.* 292: G1469–G1473.
47. Taylor, K. R., K. Yamasaki, K. A. Radek, A. Di Nardo, H. Goodarzi, D. Golenbock, B. Beutler, and R. L. Gallo. 2007. Recognition of hyaluronan released in sterile injury involves a unique receptor complex dependent on Toll-like receptor 4, CD44, and MD-2. *J. Biol. Chem.* 282: 18265–18275.
48. del Fresno, C., K. Otero, L. Gómez-García, M. C. González-León, L. Soler-Ranger, P. Fuentes-Prior, P. Escoll, R. Baos, L. Caveda, F. García, et al. 2005. Tumor cells deactivate human monocytes by up-regulating IL-1 receptor associated kinase-M expression via CD44 and TLR4. *J. Immunol.* 174: 3032–3040.
49. Misra, S., V. C. Hascall, R. R. Markwald, and S. Ghatak. 2015. Interactions between hyaluronan and its receptors (CD44, RHAMM) regulate the activities of inflammation and cancer. *Front. Immunol.* 6: 201.
50. Hu, J., R. Jacinto, C. McCall, and L. Li. 2002. Regulation of IL-1 receptor-associated kinases by lipopolysaccharide. *J. Immunol.* 168: 3910–3914.
51. Joh, E. H., and D. H. Kim. 2011. Kalopanaxsaponin A ameliorates experimental colitis in mice by inhibiting IRAK-1 activation in the NF-κB and MAPK pathways. *Br. J. Pharmacol.* 162: 1731–1742.
52. Xu, Y., L. Zhang, W. Yao, S. S. Yedahalli, S. Brand, M. Moo-Young, and C. Perry Chou. 2009. Bioprocess development for production, purification, and structural characterization of recombinant hCD83ext as a potential therapeutic protein. *Protein Expr. Purif.* 65: 92–99.
53. Huang, L., H. P. Lemos, L. Li, M. Li, P. R. Chandler, B. Baban, T. L. McGaha, B. Ravishankar, J. R. Lee, D. H. Munn, and A. L. Mellor. 2012. Engineering DNA nanoparticles as immunomodulatory reagents that activate regulatory T cells. *J. Immunol.* 188: 4913–4920.
54. Laich, A., G. Neurauter, B. Widner, and D. Fuchs. 2002. More rapid method for simultaneous measurement of tryptophan and kynurenine by HPLC. *Clin. Chem.* 48: 579–581.
55. Ziegler-Heitbrock, L., P. Ancuta, S. Crowe, M. Dalod, V. Grau, D. N. Hart, P. J. Leenen, Y. J. Liu, G. MacPherson, G. J. Randolph, et al. 2010. Nomenclature of monocytes and dendritic cells in blood. *Blood* 116: e74–e80.
56. Vanlandschoot, P., F. Van Houtte, P. Ulrichts, J. Tavernier, and G. Leroux-Roels. 2005. Immunostimulatory potential of hepatitis B nucleocapsid preparations: lipopolysaccharide contamination should not be overlooked. *J. Gen. Virol.* 86: 323–331.
57. Li, L., S. Cousart, J. Hu, and C. E. McCall. 2000. Characterization of interleukin-1 receptor-associated kinase in normal and endotoxin-tolerant cells. *J. Biol. Chem.* 275: 23340–23345.
58. Mytar, B., M. Wołoszyn, R. Szatanek, M. Baj-Krzyworzeka, M. Siedlar, I. Ruggiero, J. Wieckiewicz, and M. Zembala. 2003. Tumor cell-induced deactivation of human monocytes. *J. Leukoc. Biol.* 74: 1094–1101.
59. Harizi, H., M. Juzan, V. Pitard, J. F. Moreau, and N. Gualde. 2002. Cyclooxygenase-2-issued prostaglandin e(2) enhances the production of endogenous IL-10, which down-regulates dendritic cell functions. *J. Immunol.* 168: 2255–2263.
60. Stolina, M., S. Sharma, Y. Lin, M. Dohadwala, B. Gardner, J. Luo, L. Zhu, M. Kronenberg, P. W. Miller, J. Portanova, et al. 2000. Specific inhibition of cyclooxygenase 2 restores antitumor reactivity by altering the balance of IL-10 and IL-12 synthesis. *J. Immunol.* 164: 361–370.
61. Munn, D. H., and A. L. Mellor. 2013. Indoleamine 2,3 dioxygenase and metabolic control of immune responses. *Trends Immunol.* 34: 137–143.
62. Fallarino, F., U. Grohmann, and P. Puccetti. 2012. Indoleamine 2,3-dioxygenase: from catalyst to signaling function. *Eur. J. Immunol.* 42: 1932–1937.
63. Thomas, R., and P. E. Lipsky. 1994. Human peripheral blood dendritic cell subsets. Isolation and characterization of precursor and mature antigen-presenting cells. *J. Immunol.* 153: 4016–4028.
64. Kollewe, C., A. C. Mackensen, D. Neumann, J. Knop, P. Cao, S. Li, H. Wesche, and M. U. Martin. 2004. Sequential autophosphorylation steps in the interleukin-1 receptor-associated kinase-1 regulate its availability as an adapter in interleukin-1 signaling. *J. Biol. Chem.* 279: 5227–5236.
65. Kanakaraj, P., P. H. Schafer, D. E. Cavender, Y. Wu, K. Ngo, P. F. Grealish, S. A. Wadsworth, P. A. Peterson, J. J. Siekierka, C. A. Harris, and W. P. Fung-Leung. 1998. Interleukin (IL)-1 receptor-associated kinase (IRAK) requirement for optimal induction of multiple IL-1 signaling pathways and IL-6 production. *J. Exp. Med.* 187: 2073–2079.
66. Albrecht, V., T. P. Hofer, B. Foxwell, M. Frankenberger, and L. Ziegler-Heitbrock. 2008. Tolerance induced via TLR2 and TLR4 in human dendritic cells: role of IRAK-1. *BMC Immunol.* 9: 69.
67. Abdollahi-Roodsaz, S., L. A. Joosten, M. F. Roelofs, T. R. Radstake, G. Matera, C. Popa, J. W. van der Meer, M. G. Netea, and W. B. van den Berg. 2007. Inhibition of Toll-like receptor 4 breaks the inflammatory loop in autoimmune destructive arthritis. *Arthritis Rheum.* 56: 2957–2967.
68. Shimamoto, A., A. J. Chong, M. Yada, S. Shomura, H. Takayama, A. J. Fleisig, M. L. Agnew, C. R. Hampton, C. L. Rothnie, D. J. Spring, et al. 2006. Inhibition of Toll-like receptor 4 with eritoran attenuates myocardial ischemia-reperfusion injury. *Circulation* 114(Suppl.): I270–I274.
69. Shen, W., Y. Gao, B. Lu, Q. Zhang, Y. Hu, and Y. Chen. 2014. Negatively regulating TLR4/NF-κB signaling via PPARα in endotoxin-induced uveitis. *Biochim. Biophys. Acta* 1842: 1109–1120.
70. Biswas, A., J. Wilmanski, H. Forsman, T. Hrncir, L. Hao, H. Tlaskalova-Hogenova, and K. S. Kobayashi. 2011. Negative regulation of Toll-like receptor signaling plays an essential role in homeostasis of the intestine. *Eur. J. Immunol.* 41: 182–194.
71. Harizi, H., and N. Gualde. 2006. Pivotal role of PGE2 and IL-10 in the cross-regulation of dendritic cell-derived inflammatory mediators. *Cell. Mol. Immunol.* 3: 271–277.
72. Deng, C., C. Radu, A. Diab, M. F. Tsen, R. Hussain, J. S. Cowdery, M. K. Racke, and J. A. Thomas. 2003. IL-1 receptor-associated kinase 1 regulates susceptibility to organ-specific autoimmunity. *J. Immunol.* 170: 2833–2842.
73. Kobayashi, K., L. D. Hernandez, J. E. Galán, C. A. Janeway, Jr., R. Medzhitov, and R. A. Flavell. 2002. IRAK-M is a negative regulator of Toll-like receptor signaling. *Cell* 110: 191–202.
74. Patel, S., S. Vetale, P. Teli, R. Mistry, and S. Chiplunkar. 2012. IL-10 production in non-small cell lung carcinoma patients is regulated by ERK, P38 and COX-2. *J. Cell. Mol. Med.* 16: 531–544.
75. Sandanger, Ø., L. Ryan, J. Bohnhorst, A. C. Iversen, H. Husebye, Ø. Halaas, L. Landrø, P. Aukrust, S. S. Frøland, G. Elson, et al. 2009. IL-10 enhances MD-2 and CD14 expression in monocytes and the proteins are increased and correlated in HIV-infected patients. *J. Immunol.* 182: 588–595.
76. Obermajer, N., and P. Kalinski. 2012. Generation of myeloid-derived suppressor cells using prostaglandin E2. *Transplant. Res.* 1: 15.
77. Obermajer, N., R. Muthuswamy, J. Lesnock, R. P. Edwards, and P. Kalinski. 2011. Positive feedback between PGE2 and COX2 redirects the differentiation of human dendritic cells toward stable myeloid-derived suppressor cells. *Blood* 118: 5498–5505.
78. Fujigaki, S., K. Saito, K. Sekikawa, S. Tone, O. Takikawa, H. Fujii, H. Wada, A. Noma, and M. Seishima. 2001. Lipopolysaccharide induction of indoleamine 2,3-dioxygenase is mediated dominantly by an IFN-gamma-independent mechanism. *Eur. J. Immunol.* 31: 2313–2318.
79. Akdis, C. A., and K. Blaser. 1999. IL-10-induced anergy in peripheral T cell and reactivation by microenvironmental cytokines: two key steps in specific immunotherapy. *FASEB J.* 13: 603–609.
80. Schwartz, R. H. 2003. T cell anergy. *Annu. Rev. Immunol.* 21: 305–334.